CFD Analysis and Optimization of Abrasive Flow Machining

A thesis Submitted in partial fulfilment of the requirements for the award of the degree of

Master of Technology
In
Mechanical Engineering
(Production Engineering)
By

Shakti Ranjan Garanayak
(211ME2348)

Under The Guidance of

Prof. K. P. Maity

Department of Mechanical Engineering
National Institute of Technology Rourkela
Orissa -769008, India
May 2013

CFD Analysis and Optimization of Abrasive Flow Machining

A thesis Submitted in partial fulfilment of the requirements for the award of the degree of

Master of Technology
In
Mechanical Engineering
(Production Engineering)
By

Shakti Ranjan Garanayak
(211ME2348)

Under the guidance of

Prof. K. P. Maity

Department of Mechanical Engineering
National Institute of Technology Rourkela
Orissa -769008, India
May 2013

National Institute of Technology

Rourkela

CERTIFICATE

This is to certify that the thesis entitled **— CFD analysis and Optimization of Abrasive Flow Machining** submitted to the National Institute of Technology, Rourkela (Deemed University) by **Shakti Ranjan Garanayak Roll No. 211ME2348** for the award of the Degree of **Master of Technology** in Mechanical Engineering with specialization in**—Production Engineering** is a record of bonafide research work carried out by him under my supervision and guidance. The results presented in this thesis has not been, to the best of my knowledge, submitted to any other University or Institute for the award of any degree or diploma. The thesis, in my opinion, has reached the standards fulfilling the requirement for the award of the degree of Master of technology in accordance with regulations of the Institute.

Place: Rourkela

Date

Dr. K. P. Maity
Professor
Department of Mechanical Engineering
National Institute of Technology, Rourkela

DEDICATED TO

MY DEAREST

JHUMI

Acknowledgement

I express my deep sense of gratitude and indebtedness to my thesis supervisor Dr. K. P. Maity, Professor and Head on Department of Mechanical Engineering for providing precious guidance, inspiring discussions and constant supervision throughout the course of this work. His timely help, constructive criticism, and conscientious efforts made it possible to present the work contained in this thesis.

I express my sincere thanks to Mr. Alok Ranjan Biswal, Ph.D scholar and Dillip Bagal, Research Scholar and Mr. Abhijeet Majumdar, Technical Assistant in Production Engineering lab, for their support during the project work. I am also thankful to all the staff members of the department of Mechanical Engineering and to all my well-wishers for their inspiration and help. I am also thankful to my classmates Ved Prakash Kishor, Poorna chandu karuturi, Debasis Nayak , Neelam Verma for their help during my project work.

I feel pleased and privileged to fulfil my parent's ambition and I am greatly indebted to them for bearing the inconvenience during my M Tech. course.

Date

Shakti Ranjan Garanayak

Roll No - 211ME2348

ABSTRACT

This study deals with a new approach to understand the micro finishing of abrasive flow machining process in which computational fluid dynamics is used to simulate the forces. Mathematical modelling is applied to model the micro finishing operation. The study is conducted to compare the simulated results with the existing experimental results. A flexible polishing tool comprising polishing medium is used to carry out the analysis. The relative motion between the polishing medium and the workpiece surface provides the required finishing action. In the present work a two dimensional computational fluid dynamics simulation inside the workpiece fixture is performed to evaluate the axial and radial stresses developed due to the flow of polishing medium. The present study also develops optimization for AFM process of Al. alloy using response surface method. It is found that all the three machining parameters and some of their interactions have significant effect on outputs considered in the present study. Finally, an attempt has been made to estimate the optimum machining conditions to produce the best possible output within the experimental constraints.

Keywords: AFM, Simulation, RSM, ANOVA

Contents

LIST OF FIGURES

LIST OF TABLES

Chapter 1

Introduction of AFM

Precision and Ultra finishing process represents a critical and expensive phase of the overall production process. Manufacturing of precision parts consists a stage of final finishing operation. It is mostly uncontrollable, labour intensive and frequently involves a reasonable part of the total manufacturing cost. The functional properties such as wear resistance and power loss due to friction are influenced by surface roughness of the matching parts [1, 3].

To counter the problems such as high direct labour cost and to produce finished precision parts with specific features for finishing inaccessible areas, abrasive finishing techniques are developed. Abrasive finishing process is carried with large number of cutting edges which have indefinite orientation and geometry. Abrasive fine process are commonly employed due to their capacity of finishing various geometries of form (i.e. Flat, round etc.) with desired dimensional accuracies and surface finish [1, 6].

1.1 OVERVIEW OF TRADITIONAL FINISHING PROCESS:

Before discussing advanced finishing process, it is beneficial to understand the material removal mechanism commonly adapted in conventional finishing process. Grinding, honing, microhoning are the examples of conventional abrasive finishing process. Multi point cutting tool in the form of abrasive cutting particles are used in these Method.

In all these finishing process the particle workpiece interaction involves one or more of the basic material removal. i.e. cutting, ploughing,sliding/friction. Mostly cutting is a material removal process, ploughing is a material displacement process and sliding is a material modifiacation process. The intensity of material deformation and change in surface roughness depends upon the amplitude of forces and the number of active abrasive cutting edges in abrasive finishing process [1-3].

In grinding process a grinding wheel made up of large abrasive cutting points is used. Grinding is more effective in removing material than finishing surfaces due to random

distribution of abrasive particles. Finishing of complex parts is difficult and requires expensive shaped grinding wheel.

In lapping process the surfaces produced are smoother and more accurate than produced in the grinding process. Loose abrasive slurry is used between the work piece and the gap. Lapping is used at very low abrading pressure and a slow movement of lap increases the surface finish and the dimensional accuracy is achieved.the shapes of the surfaces generally worked in lapping are limited to elementary forms such as cylindrical and flat.

Honing is considered to be the smoothening process than material removal process. This process normally works on low cutting velocity, low pressure and large area of contact. A solid tool made up of abrasive is used in this process. The tool is having low reciprocating motion and rotates with high speed inside the workpiece. Thus this process produce scratch pattern on the work piece surface [3, 5].

Super-finishing is a low velocity abrading method. A very fine abrasive stick is mounted on a holder and pressed with light spring pressure against the workpiece surface in this process. The work piece is given reciprocating motion and the stick is given feed or oscillating motion [4, 6].

1.2 Advanced abrasive finishing process:

The available traditional processes are unable of producing desired nano/micro level finishing.also these require high expensive equipment, more time consuming and economically incompetent.

Hence to meet the present demand of industries new abrasive fine finishing processes are developed. Abrasive flow machining is one of the processes with wide range of application.Other processes are MAF, MRF and MFP where the control of performance is done by the use of magnetic field [4, 5].

1.2.1 Magnetic Abrasive Finishing (MAF):

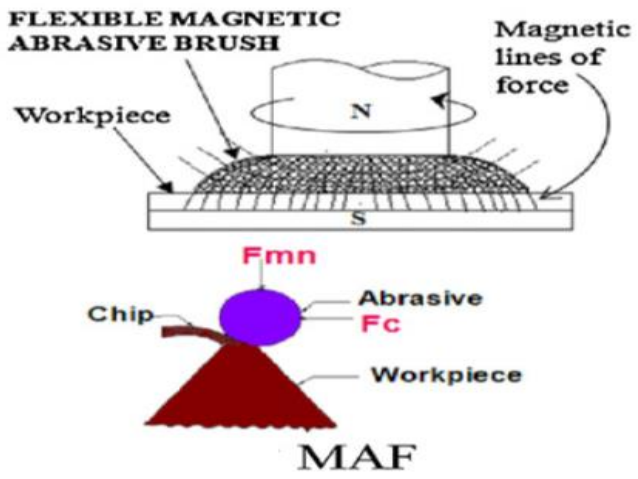

Figure No. 1: Magnetic abrasive flow machining

MAF is mostly used for the finishing process of metals and ceramics. A good quality internal and external finishing in both cylindrical and flat surfaces is produced in this process.

Fig.1 shows a typical MAF process in which the workpiece to be finished is situated between two magnetic poles and the gap between the workpiece and magnetic poles are filled with abrasive powder. This abrasive powder is used for surface and edge cutting. A mirror type image is produced and the burrs are removed without changing the shape because the magnitude of machining force used is very low [1-6].

1.2.2 Magneto-Rheological Finishing (MRF):

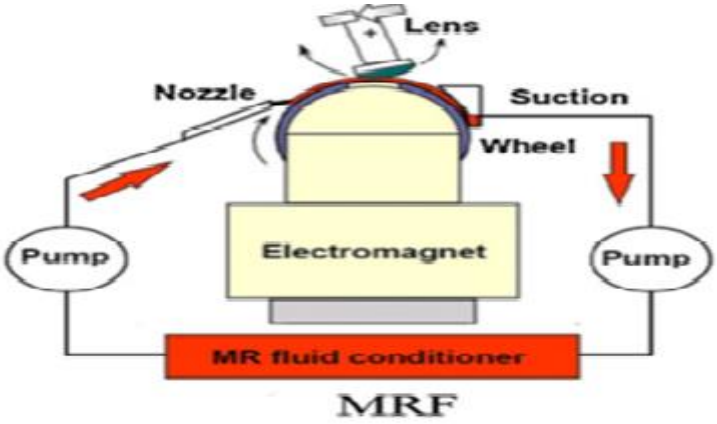

Figure No. 2: Magnetic Rheological finishing

The MRF process uses a smart fluid known as Magneto Rheological fluid. These fluids are suspension of magnetic particle and finishing abrasive which have the influence in cutting the material proportional to magnetic strength.

The stiffened region produces a transient work zone or finishing spot by applying the magnetic field in the gap. Surface smoothening and removal of sub-surface damage, and figure correction are done through rotating the lens on a spindle at a constant speed while sweeping the lens about its radius of curvature through the stiffened finishing zone [1-4].

1.2.3 Magneto-rheological flow polishing:

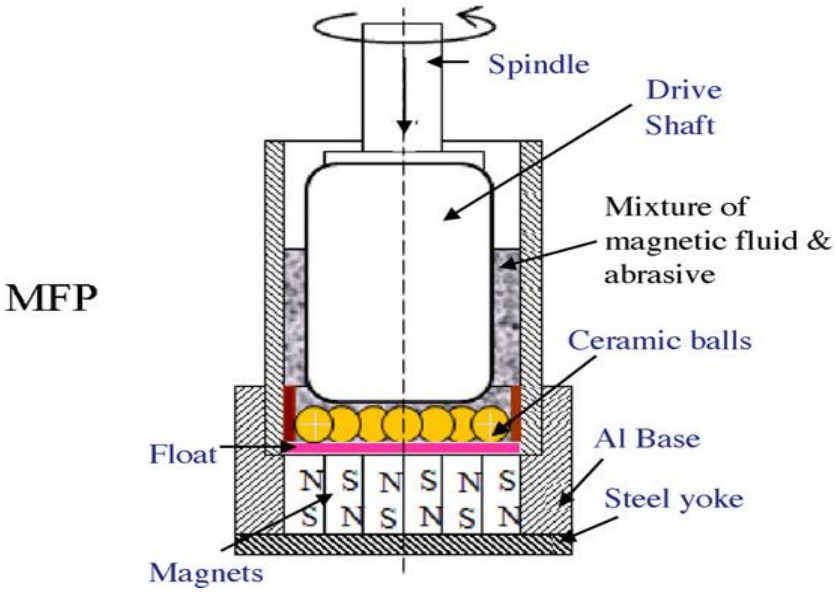

Figure No.3: Magneto rheological flow polishing

The MFP method is based on the Ferro-hydrodynamic conduct of a magnetic fluid that levitates balls, abrasives and float pad. Because this levitation force is proportional to the magnetic field gradient. It can be very cost effective and reliable method for finishing materials with high precision for brittle materials with flat and spherical shapes [1].

Compared to other finishing methods polishing time in MFP is very low. Hence this process is very cost-effective and the surface formed has little or no defects.This process can be automated as well.

1.3 Limitation of Magnetic field assisted finishing processes [2-6]:

- To provide the uniform magnetic force, magnet should be made converse to the complex surface.
- Due to their high density, abrasive particle get sedimented .
- Variation in magnetic field during finishing operation happens, due to the presence of chips and non-uniformly distributed abrasive particle.
- For finishing thick work pieces these processes cannot be applied, because of the high thickness of workpiece the magnetic field becomes quite low in finishing region compared to top surface where it is applied.

1.4 Abrasive Flow Machining Process (AFM):

Abrasive Flow Machining was developed by Extrude Hone Corporation, USA in 1960. AFM can be regarded as a process of generating a self –formingly tool that correctly removes the workpiece material and finishes those areas which are restricted to the medium flow. AFM technique is used for deburring, edge contouring and surface finishing. It is capable of finishing regions which are difficult to reach by flowing abrasive by mixing with polymer of special rheological properties. AFM produces uniform, repeatable and predictable results on a notable range of finishing operation. Normally the properties of carrier in AFM process play an important role. They should be visco-elastic and non-sticky in nature. Aluminium Oxide, Silicon Carbide, Boron Carbide and Diamond are commonly used abrasive grains in AFM process [1-6].

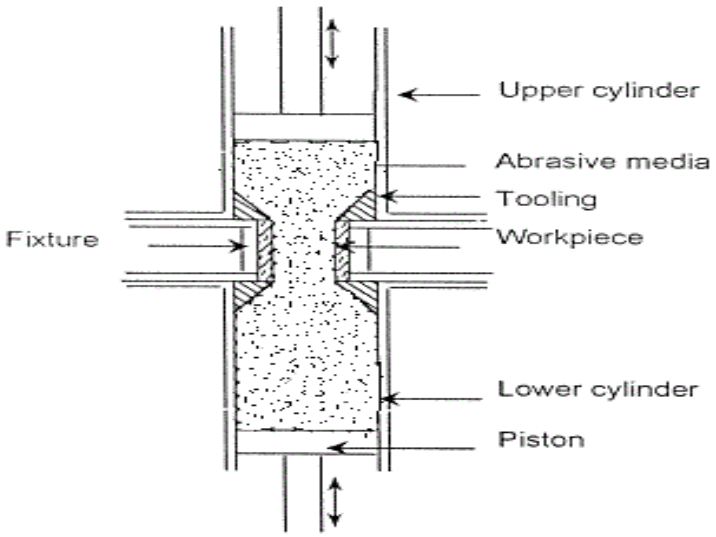

Figure No. 4: Abrasive Flow machining

1.4.1 Working principle:

In abrasive Flow Machining process, polymer based on visco-elastic material matrix is mixed with abrasive particle and additives which called as the medium, which is extruded back and forth in two vertically opposed cylinder .While extruded through the passage formed by the workpiece and tooling, this medium tries to finish the workpiece surface selectively. Tooling plays the important role in this process. So tooling or fixture design should be done carefully [1-7].

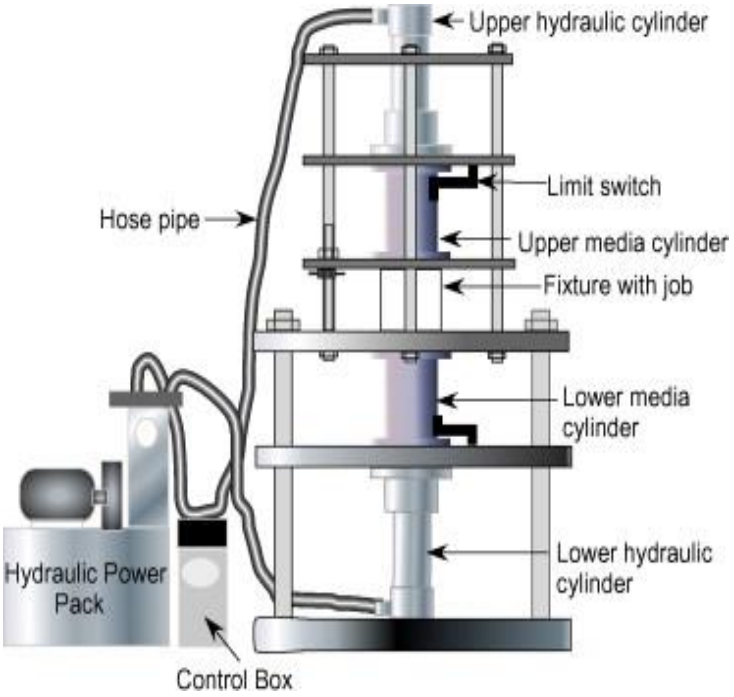

Figure No. 5: Schematic diagram of AFM

Because of the flow through the restricted passage of workpiece region, the polymer chain holds the abrasive particle flexibly and moves them around in the direction of extrusion pressure. Hence the medium acts as a multi-point cutting tool and starts abrading the work piece surface.

Extrusion pressure, Number of cycle, work-piece initial surface roughness and medium viscosity are the significant variable parameter having an impact on final surface roughness. The viscoelastic medium moves along the direction of applied pressure with axial velocity and axial force when sufficient extrusion pressure is applied. On the application of

extrusion pressure due to elastic component of medium, it exerts radial force which is responsible for penetration of the abrasive on the work-piece. Axial force is responsible for removal of material in the form of micro-chips by shearing the indented abrasive particle in the axial direction. This method is applicable for different types of abrasive finishing process.

1.4.2 Abrasive Flow Machining System [1-4]:

AFM system consists of three different elements i.e. Machine, Tooling and Medium.

Machine: Depending upon capacity AFM machine is available in various sizes and designs. It consists of frame structure, medium cylinder, hydraulic cylinder and control system. Generally the working pressure ranges from 1Mpa to 16Mpa.

Tooling: The purpose of Tooling or fixture is to locate and hold the workpiece in position as well as to direct the flow of medium. The tooling is designed in such a way that, it restricts the flow of medium in the region where the material removal is needed.

Medium: It is a mixture of polymer, rheological aditives and abrasive particles. Polyborosilaxane polymer is mostly used in this process. Other kind of polymers also can be used according to the workpiece. Silicon carbide, boron carbide, alumina or diamonds are the commonly abrasive particle used. The polymer acts as a binder and to transmit extrusion pressure in different direction. While the function of abrasive particle is to abrade the workpiece surface when the medium flows over the restricted passage. The rheological properties of the medium are governed by its performance [35, 36].

AFM can be differentiated from other process in a way that, it is possible to control and select the intensity and location of abrasion through fixture design, medium selection and process parameter.

1.4.3 Features of AFM [3-6]:

- In AFM abrasion of workpiece can takes place where the flow is restricted.
- To deburr and polish any inaccessible and complex areas is possible by forcing the abrasive medium into it.
- AFM maintains precision, consistency and flexibility to a wide range of application.
- It can polish any where that air, liquid, or fuel flows.
- It is possible to achieve high level of surface finish and accuracy.

1.4.4 Application of AFM [1-4]:

- Adjusting air flow resistance of blades, vanes, combustion liners and diffusers.
- Improving airfoil surface conditions on compressors and turbine sections components.
- Improve the mechanical fatigue strength of discs, edge finishing of holes and attachments to blades, hubs and shafts with controlled polish.
- Finishing accessory parts such as fuel spray nozzles, fuel control bodies and bearing components.

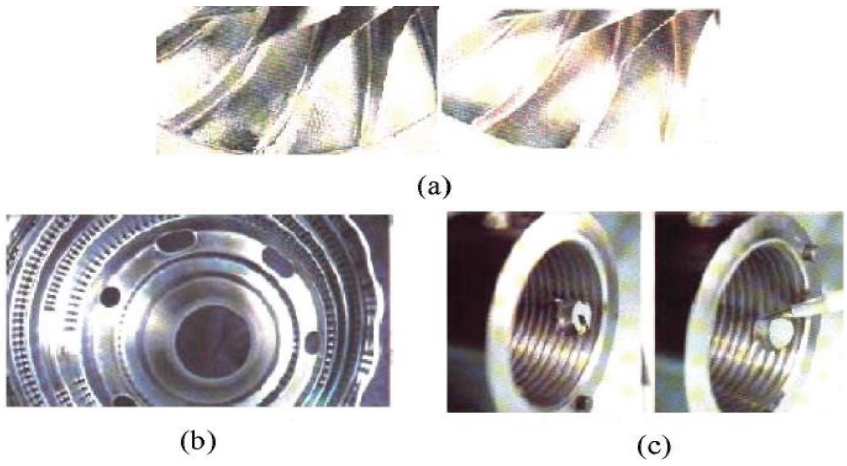

Figure No. 6: (a) Surface finish of cast blades, (b) deburring of cooling holes in turbine blades, (c) finishing of intersections

Figure No. 7: AFM of some complex holes

Figure No.8: AFM of complex cylindrical holes

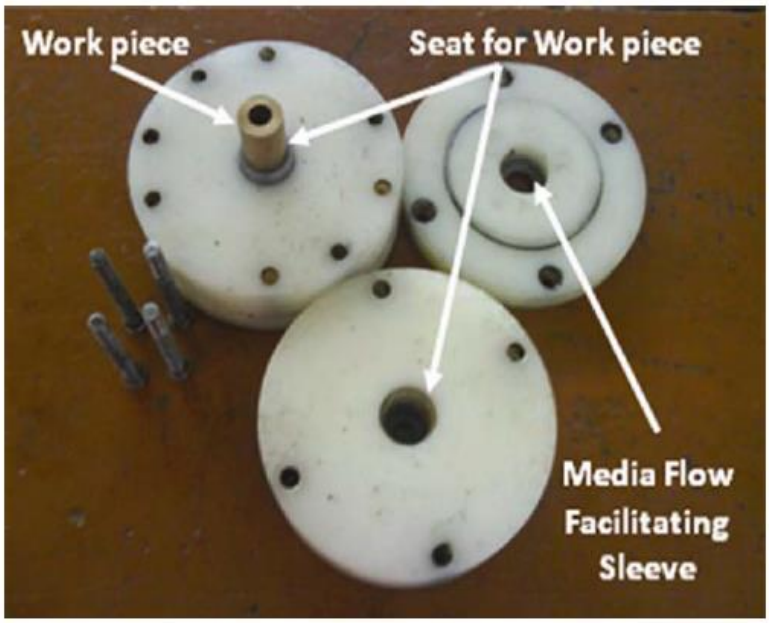

Figure No. 9: Tooling for AFM

It is a well- known fact in automobile engineering, that it is very difficult to attain the surface finish in the internal passageway of intake ports due to complex shape. The surface finish is improved by applying AFM process to intake and exhaust manifold.

.

Chapter 2

Literature Review

Abrasive flow machining is a micro/nano finishing process on which a great amount of research work have been done in the form of research papers, book chapters and patents. A brief review of same has been presented in this section. This review has been divided into further sub-sections as follows.

2.1 AFM process mechanism:

Rhodes found that [11-14] in AFM process depth of cut by abrasive particle depends on size, relative hardness, sharpness of abrasive particle and extrusion pressure. He stated that medium viscosity plays a vital role in finishing action. The medium flow pattern which affects finishing characteristics depends on machine settings, medium formulation and tooling configuration. In the restricted passages the viscosity of medium increases temporarily and gives nearly pure extrusion of the medium. For abrading walls of large passages high viscosity medium was recommended and low viscosity medium was found suitable for radiusing edges and for finishing slender passages.

Experimental study by Przyklenk [15] suggested that, the material removal capacity of high viscous medium was around 300 times greater than that of low viscous base medium. The important factors that influence stock removal and medium velocity are abrasive percentage concentration, abrasive size and viscosity of the medium.

Williams and Rajurker [16-21] conducted additional experiments to study the effect of extrusion pressure and medium viscosity on material removal and surface finish. Loveless et.al.[20] concluded through their experiments that initial surface roughness and viscosity significantly influence the percentage surface finish improvements.

Later Jain et.al. [2-4] Suggested that the abrasive concentration and mesh size on medium viscosity at different temperatures. They made-up a capillary rheometer and conducted experiments to study rheological properties of abrasive loaded polymeric medium. They mentioned that increase in medium viscosity leads to decrease in surface roughness.

It is determined by many researchers that viscosity of polymeric medium is a vital parameter which affect AFM performance.

2.2 Surface finish and material removal mechanism:

Rhodes [11-14] investigated through experiments that, the basic principle of AFM process and identified its process control variables. He stated that when the medium is suddenly forced through the restricted passages its viscosity rises. Major material removal is observed when the medium is thickened. The abrasion efficiency during AFM depends on tooling and fixtures. Higher volume of the medium will result in interaction at more number of times between abrasive particle and the work piece; hence more abrasion per number of cycle will take place. For uniform finishing and small radius of edges slow medium flow rates are suitable .while high flow rate will result in large radii. Low viscosity medium should be used to get better result in comparison to high viscosity medium. If radiusing and deburring along edges of passageway is also to be done along finishing then. Flow pattern medium depends on its slug flow speed, rheology and passage size. Medium flow rate depends on size and number of passage to be processed.

Perry [35] obtained some principle and industrial application of the AFM. i.e. precision deburring, edge contouring, sufacefinsh and removal of thermal recast layers. William and Rajurker [17-19] used full factorial design for research and calculated the effect of medium viscosity and extrusion pressure on material removal and surface finish. Metal removal results shows that the viscosity main effect was significant while the pressure main effect is not so important. Jainet.al. [3-4] stated that the initial surface roughness and hardness of the workpiece affect the material removal during the AFM process. For the case of softer metal as compared to harder metal, Material removal and change in surface roughness value were found to be higher. With the increase of percentage concentration of abrasive in the medium material removal rate increases. They determined that among all the process parameter studied, the leading parameter is abrasive concentration followed by abrasive size and number of cycles.

The types of machining process used to prepare the workpiece before the AFM plays a significant role in process performance [6]. As compared to turned and milled surface wore

EDM surfaces are found to be more suitable for AFM process. Because the machining surfaces produces different surface textures and contours.

Davis and Fletcher [22] described the relationship between the number of cycles, temperature, and pressure drop and across the die which are dependent upon the type of polymer as well as the abrasive concentration used. An increase in temperature results in decrease in viscosity and increase in medium flow rate. With increase in finishing time the medium temperature increases that changes medium viscosity. The change in temperature is partly due to the internal shearing of the medium and the abrasion process.

2.3 Medium composition and its rheology:

The medium is a main element in the AFM process and it is able to precisely abrade the selected areas along which it flows. The medium is included of a base carrier, abrasive particle and additives [24] .The base carrier is a high molecular weight material with dominant elastic properties and low viscosity. Rheological additives such as plasticizers and softeners are mixed to it, to improve viscous properties of the base carrier. The plasticizer as well as softeners are low molecular weight materials and can easily diffuse in high molecular weight base polymer carrier when mixed [26-29]. The viscosity of the medium decreases due to the diffusion of low molecular weight forces the polymer chains apart. In these mixtures Abrasive particles are held by the polymer matrix material. High viscous medium is rich in base polymer contents with a small amount of plasticizer. Hence high viscosity medium possess relatively high elastic components and hence this medium yield high rate of material removal per cycle. And low viscosity medium behaves like fluid that effortlessly passes through very small diameter holes [25-27].

Winfield B Perry [US patent no: 6132482] developed abrasive liquid slurry for polishing and radiusing a micro-hole. Liquid abrasive slurry consists of polymer (polyboro-siloxane) +low viscous naphthenic mineral oil + rheological additives + abrasive particles (SiC). Kukreja and Rakesh [23] established a new AFM medium consists of ethylene propylene dyene-moner, naphthenic oil, toluene, abrasive particle. To dissolve the compound and to decrease the viscosity Toluene is added.

Randen et.al. (US patent no: 6918937) developed abrasive concentration for orbital abrasive finishing process. Composition consists of polymer carrier(polyborosiloxane) (starting viscosity of $(5 \times 103\ to\ 5 \times 105\ c.p)$,optical inert filler + abrasives(diamonds)+ optional plasticizing lubricant[30].Viscosity can be increased by two ways, one is by increasing the share of the abrasive particle in the medium and the other is by using high viscous polymer.

Fletcher et.al. [22] stated the viscosity of polyborosiloxane medium without abrasive particle and got it as pseudo plastic in nature. Material removal rate and surface finish in AFM are significantly affected by the medium viscosity which substantially decreases even with a small increase in temperutre.medium viscosity increases with an abrasive particle concentration and it decreases with abrasive particle size.

Abrasive particle action in AFM process depends upon rheological properties of the medium. The viscosity which plays an important role in finishing operation is a rheological property. This allows the abrasive particle to selectively and controllably abrade surface over which it flows. Where the flow path is restricted and travels with high velocity the abrasion is high [30].

2.4 Active Grains:

William and Rajurkar [18-21] recommended that the number of can be obtained by using the pseudo-frequency associated with the primary root from the data dependent system model of the AFM generated surface profiles. The number of dynamic active grains over a unit area of extrusion passage is achieved by

C_d =frequency x time for one stroke/cross-sectional area

Jain [18] found the active grain density by counting the number of shining grains over the medium surface. They described the active grain density increases with the concentration and abrasive mesh size.

2.5 Force and Specific Energy:

To evaluate the forces on a single abrasive grain in AFM process, Jain and Jain [19] presented a force analysis based on abrasion theory. From the analysis they projected the specific energy AFM and compared it with the specific energy in fine grinding and concluded

that the magnitude of specific energy in AFM could be used to predict the mechanism involved in surface generation.

2.6 Representation of surface roughness:

Jain [5] suggested that there is a necessity for systematic procedure for the selection of a set of parameters to represent the surface roughness which fulfils the following basic conditions.

1. Define the geometric feature of the surface.

2. Enable precise interpretation.

3. Measurable by commonly available instruments.

4. Applicable in research

Jain [4, 5] determined that, in production inspection high quality surface should be tested by checking the parameters such as CLA value and mean slope of profile. He concluded that for stable and well controllable production process the second parameters need not to be inspected regularly.

2.7 Recent advances on AFM processes:

Some of the recent advances in the AFM process are discussed below.

2.7.1 Magnetic AFF process:

Singh and Shan [10] used the medium made of silicon polymer base carrier, hydrocarbon gel and magnetic abrasive particle in Magnetic AFF set up. Magnetic field is applied around the workpiece and observed that magnetic field affects the material removal rate and surface roughness.

2.7.2 Electro-chemically assisted Abrasive flow machining process:

Electro-chemically assisted abrasive flow machining process which uses polymeric electrolyte such as gelated polymers and water gel as base carrier. The conductivity of electrolyte employed in ordinary chemical machining process is many times lower than the

ion conductivity of electrolyte. The conductivity decreases even more with the addition of inorganic to electrolyte. The polymeric electrolyte medium forced the through small inter electrode gap. This in turn results in greater flow resistance of polymeric electrolyte which takes the form of semi-liquid paste. In flat surfaces experimental investigation have been carried out.

2.7.3 Ultrasonic flow polishing:

Ultra-sonic flow polishing is combination of AFM and Ultra-sonic machining. The medium pumped down the centre of the ultrasonically energized tool, flow radially relative to the axes of the tool.

2.7.4 Spiral polishing:

In Spiral polishing a spiral fluted screw is placed at the centre of the hole in workpiece to be finished. Using external energy source the screw is rotated. The rotational motion of the screw lifts the medium from lower medium cylinder to upper medium cylinder and tries to finish the hole while passing through it.

2.7.5 Centrifugal force assisted Abrasive flow machining process:

In this process a centrifugal force generating tiny rod is placed at the centre of the medium slug in the workpiece finishing region.in this region the rod strikes the abrasive particle that come in contact with it. The angle of moving of abrasive particle depends on rotational speed and shape of the rod. The placing of rod in the centre and providing rotation to it increase the finishing rate by 70-80%.

2.7.6 Drill-bit guided Abrasive flow finishing process:

In a drill-bit guided AFF process, a freely rotatable drill bit is placed with the help of a special fixture plates in the workpiece finishing zone. By the combination of medium reciprocation, medium flow rate through the drill bit flute and scooping flow across the flute the actual path of movement of abrasive particle decided. This makes the abrasive particle to move in an inclined motion rather than to move in a straight-line motion. Turbulence at the centre is also causes frequent reshuffling of abrasive particle. Thus material removal rate and finishing actions well as surface roughness is also enhanced.

2.8 Limitation of AFM:

- The rate of finishing is low.
- The rheological properties of the medium degrade due to long finishing time, and thus the finishing ability of the medium reduces in the latter half of the useful life.
- The probability of reshuffling of abrasive particle is less in AFM process and abrasive particle at the centre of the medium slug won't take part in finishing operation.
- In commercially existing AFM machine the medium cylinder are in uni-axis, so finishing of complex surfaces needs complex tooling which increases the production cost.
- In the process of Spiral polishing, CFAAFM, DBGAFM create motion at the centre of the medium slug. This may not be able to force the abrasive particle to reach up to the finishing zone.

2.9 Objective of the present work:

In the present work attempts are made in finishing of homogenous Aluminium alloy material. The main objective of the thesis is as follows.

- Develop a CFD simulation of the Abrasive flow Machining with proper boundary conditions in the Aluminium-alloy work piece and find out the axial and radial stresses.
- Predict the material removal rate.
- Optimize the various outputs such as axial stress, radial stress and depth of indentation from the input parameters like volume fraction, extrusion pressure and inlet velocity.

Chapter 3

Simulation of AFM

In the abrasive flow machining process discussed above, it is needed to make experiments for output results. Different input parameters are required for every output. Which is very time consuming and cost effective and also not accurate due to the inevitable error in machine parts. So it is difficult to get the optimum input parameter for better result.

So the analysis of Abrasive flow machining numerically by using the software CFD (FLUENT) of ANSYS13 is done. Then by getting the outputs and putting those into the equations got the required results.

3.1 Computational Fluid Dynamics (CFD):

CFD or computational fluid dynamics forecasts quantitatively, when fluid are flowing, frequently with the difficulties of concurrent flow of phase change (e.g. melting, freezing, boiling), chemical reaction, and mechanical drives (e.g. Fans, pistons etc.), Stresses and displacement of occupied or neighbouring solids. Computational fluid dynamics (CFD) is the branches of fluid mechanics that uses numerical methods and algorithms to resolve and analyse problems that involve fluid flows. Computers are used to get huge calculations needed to simulate the interaction of fluids and gases with the intricate surfaces used in engineering. Even with basic equations and high-speed supercomputers, only approximate solutions can be attained in many cases. On successful research, however, may produce software that advances the correctness and speed of intricate simulation conditions such as turbulent flows. Initial verification of such software is often performed using a wind tunnel with the final validation coming in flight test. To treat a continuous fluid in a discretized way on a computer is the most vital thing in CFD. Computational fluid dynamics forecasts quantitatively, when fluid is flowing, frequently with the difficulties of concurrent flow of phase change (e.g. melting, freezing, boiling), chemical reaction, mechanical drives (e.g. Fans, pistons etc.) Stresses and displacement of occupied or neighbouring solids. Computational fluid dynamics (CFD) is the branches of fluid mechanics that uses numerical methods and algorithms to resolve and analyse problems that involve fluid flows. We use

computers to get huge calculations needed to simulate the interaction of fluids and gases with the intricate surfaces used in engineering. Even with basic equations and high-speed supercomputers, only approximate solutions can be attained in many cases. On successful research, however, may produce software that advances the correctness and speed of intricate simulation conditions such as turbulent flows. Preliminary verification of this software is frequently done using a wind tunnel with the last validation coming in flight test. One technique is to discretize the three-dimensional domain into small cells to generate a volume mesh or grid, and then by applying an appropriate algorithm in solving the equations of motion (for inviscid Euler equations and for viscous flow Navier- Stokes equations). Also this type of mesh can be either irregular (for Example consisting of triangles in 2D, or pyramidal solids in 3D) or regular. If we chooses not to continue with a mesh-based technique, a number of substitutes exist, notably Smoothed particle hydrodynamics (SPH), a Lagrangian technique of solving fluid problems, Spectral methods, a technique where the equations are projected onto basis functions like the sphere-shaped harmonics and Chebyshev polynomials, which simulates a matching mesoscopic arrangement on a Cartesian grid, in place of solving the macroscopic system. When all of the applicable length scales can be determined by the grid then we can directly solve the laminar. One technique is to discretize the three-dimensional domain into small cells to generate a volume mesh or grid, and then by applying an appropriate algorithm in solving the equations of motion (for inviscid Euler equations and for viscous flow Navier- Stokes equations). Also this type of mesh can be either irregular (for Example consisting of triangles in 2D, or pyramidal solids in 3D) or regular. If we chooses not to continue with a mesh-based technique, a number of substitutes exist, notably Smoothed particle hydrodynamics (SPH), a Lagrangian technique of solving fluid problems, Spectral methods, a technique where the equations are projected onto basis functions like the sphere-shaped harmonics and Chebyshev polynomials, which simulates a matching mesoscopic arrangement on a Cartesian grid, in place of solving the macroscopic system. When all of the applicable length scales can be determined by the grid then we can directly solve the laminar flows and turbulent flows by Navier- Stokes equations. However, the range of length scales suitable to the problem is greater than even today's immensely parallel computers can model. In these cases, turbulent flow simulations need the introduction of a turbulence model. In many examples, to deal with these scales we need large eddy simulations (LES) and the Reynolds-averaged Navier-Stokes equations (RANS) formulation, with the k-ε model or the Reynolds stress model. The Navier-Stokes equations solve other equations. These other equations can comprise those relating species concentration (mass

transfer), chemical reactions, heat transfer, etc. for the simulation of more complex cases connecting multi-phase flows (e.g. liquid/gas, solid/gas, liquid/solid), non-Newtonian fluids (Such as blood), or chemically reacting flows (such as combustion) More advanced codes are required.

3.1.1 DISCRETIZATION METHODS IN CFD:

The steadiness of the chosen discretization is generally known numerically rather than analytically as with simple linear problems. We must be cautious to make sure that the discretization is handling discontinuous solutions elegantly. The Euler equations and Navier-Stokes equations both admit shocks, and interaction surfaces.

Some of the discretization methods being used are codes, this normal method is used. On discrete control volumes.

3.1.1.1 Finite volume method (FVM):

Mostly in profitable software and research solved. FVM reorganizes the PDE's (Partial Differential Equations) of the N-S equation in the traditional form and then discretize this equation. This promises the conservation of fluxes through a specific control volume. There is no assurance that it is the definite solution though the general explanation will be conventional. Furthermore this method is subtle to distorted elements which can avoid convergence if such elements are in critical flow regions. This integration method produces a method that is integrally conventional (i.e. quantities such as density remain physically expressive.

3.1.1.2 Finite element method (FEM):

For structural analysis of solids this method is prevalent, but is also appropriate to fluids. However, special care to ensure a conservative solution for the FEM designs. For use with the Navier-Stokes equations the FEM design has been modified. It is much steadier than the FVM method, although in FEM conservation has to be taken care of. Later it is the new way in which CFD is moving. Normally steadiness/robustness of the solution is better in FEM though for some cases it might take more recollection than FVM methods.

3.1.1.3 Finite difference method:

This technique has ancient significance and is simple to program. It is presently only used in little particular codes. Current finite difference codes make use of an embedded boundary for treating complex geometries making these codes highly effective and precise. Where the solution is interpolated across each grid there are other ways to handle geometries are using overlapping-grids. The boundary employed by the fluid is divided into surface mesh in boundary element method.

Where shocks or cut-offs are present high-resolution schemes are used. the use of second or higher order numerical arrangements that do not introduces forged oscillations is needed to capture sharp changes in the solution. To confirm that the solution is total variation diminishing, this frequently requires the application of flux limiters.

3.1.2 How does CFD work:

CFD work is done by writing down the CFD codes. CFD codes are organized around the numerical algorithms that can challenge fluid problems. Inorder to run easy access to their solving power all commercial CFD packages comprise sophisticated user boundaries input problem parameters and to inspect the results.

Hence all codes comprise three key elements:

1. Pre-processing.
2. Solver
3. Post - processing.

3.1.2.1 PRE-PROCESSING:

Pre-processor contains input of a flow problem by means of an easy interface. Following conversion of this input into suitable form for use by the solver.

The actions of the user at the Pre-processing phase include:

1) Description of the geometry of the region: The computational domain. Grid generation is the subdivision of the domain into a number of lesser or no overlapping sub domains.

2) Explanation of fluid properties: The solution of a flow problem (velocity, pressure, temperature etc.) is defined at nodes inside each cell the description of suitable boundary conditions at cells that coincide with the boundary. Governing of the correctness of CFD solutions is done by number of cells in the grid. Usually, the larger numbers of cells better the solution correctness. Both the accuracy of the solution & its cost in terms of essential computer hardware & calculation time are dependent on the fineness of the grid. Efforts are on-going to improve CFD codes with a (self) adaptive meshing capability. Finally such programs will automatically refine the grid in areas of rapid variation.

3.1.2.2 SOLVER:

These are three separate streams of numerical solutions methods: finite difference, finite volume& finite element methods. In outline the numerical methods that form the basis of solver accomplishes the following steps:

1) The approximation of unknown flow variables are by means of simple functions. Discretization by replacement of the approximation into the governing flow equations and subsequently mathematical manipulations.

3.1.2.3 POST-PROCESSING:

As in the pre-processing massive amount of development work has newly taken place in the post processing field. Due to increased acceptance of engineering work stations, many of which has excellent graphics abilities, the important CFD are now equipped with multipurpose data visualization tools.

These include:

1) Domain geometry & Grid display
2) Vector plots
3) Line & shaded contour plots
4) 2D & 3D surface plots
5) Particle tracking
6) View manipulation (translation, rotation, scaling etc.)

3.1.3.1 Present study:

In the present study a two dimensional (2D) computational fluid dynamics (CFD) simulation of the medium has been carried out to calculate the axial and radial stresses developed during machining.

3.1.3.2 Governing equations:

The mathematical representation of the medium in the AFM process includes basic equations of continuity and momentum equations [8, 9].

$$\frac{\partial u_i}{\partial x_i} = 0 \tag{1}$$

$$\rho\left[\frac{\partial u_i \partial u_i}{\partial x_i}\right] = \frac{\partial \rho}{\partial x_i} + \frac{\partial}{\partial x_j}\left[\mu\left(\gamma\left(\frac{\partial u_i}{\partial x_j} + \frac{\partial u_i}{\partial x_i}\right)\right)\right] \tag{2}$$

Where ρ the density of the fluid, p is is the pressure and u_i is the flow velocity in I- direction. In the equation above the shear rate is derivable from the second invariant of the rate of deformation tensor, D_{ij} and it is given as

$$\gamma = \sqrt{2D_{ij}D_{ij}} \tag{3}$$

Where

$$D_{ij} = \frac{1}{2}\left(\frac{\partial u_i}{\partial x_j} + \frac{\partial u_i}{\partial x_i}\right) \tag{4}$$

- In the present simulation we did not consider the heat generation resulted from the viscous dissipation. But the continuity, momentum and energy equation are solved for more precise modelling.as there is a chance of affecting the viscosity because of increase of temperature.
- In this study a quasi steady state is assumed.
- The fluid is considered as incompressible.
- Modelling of the flow is done on a time averaged scale. Therefore unsteady terms resulted from the reciprocating motion is in the momentum equation are avoided.

In the present study a cylindrical work piece fixture made up of brass having internal slots in which the flat workpiece is placed.

3.1.3.3 Geometry of workpiece:

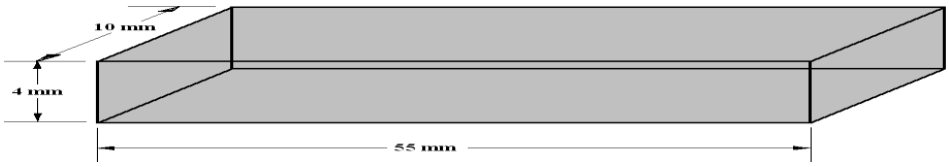

Figure No. 10 shows the workpiece with dimension

3.1.3.4 Geometry of workpiece fixture:

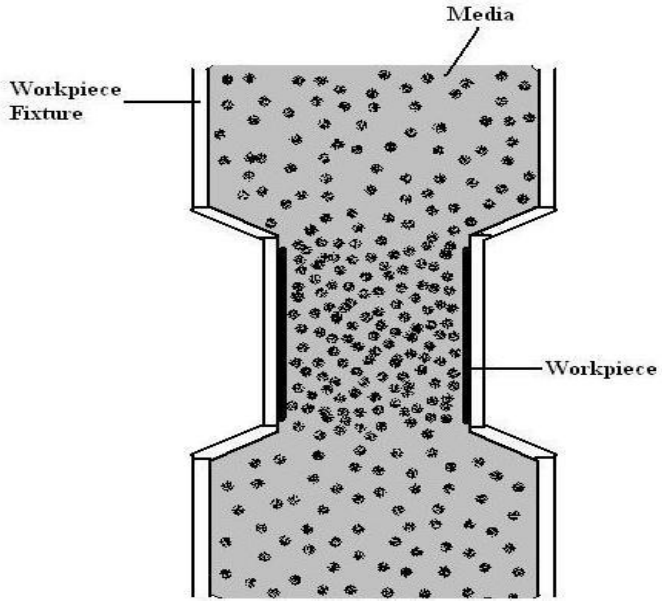

Figure No. 11: Shows the workpiece fixture

3.1.3.5 Design of work piece with fixture in Gambit:

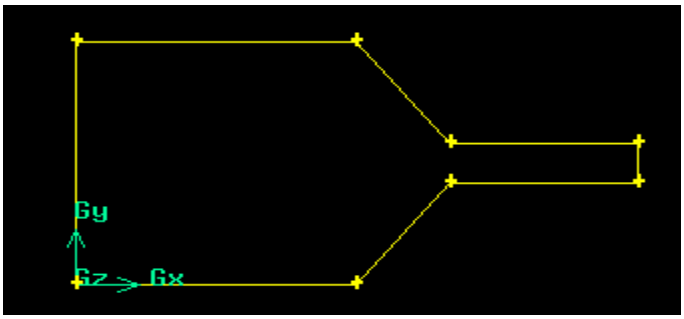

Figure No. 12: Geometry of workpiece with fixture

The design of workpiece is done by the GAMBIT software (solver 5/6).

Formulation of design through GAMBIT:

Create the vertex through the process,

Geometry command –vertex command –apply

Then create the face by,

Geometry command-face command-apply

As we are making two dimensional figure then no need to create the volume.

Then create the mesh by,

Mesh command-edge command-interval count-spacing-apply

Mesh command-face command-element (quadr)-interval count-spacing-apply

Then create the zone name by,

Zone command-specify boundary type command-name-type-apply

Then specify continuum type. After that save the mesh file and export it to the fluent (ANSYS 13).

3.1.3.6 Meshed diagram of workpiece with fixture:

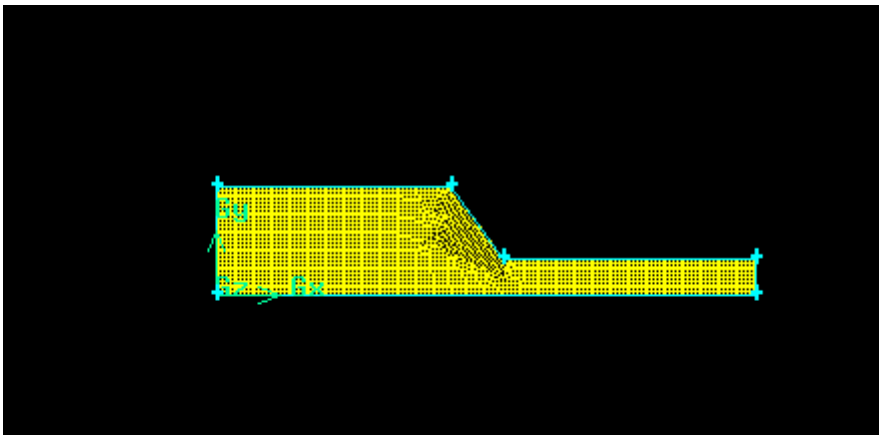

Figure No. 13. Meshed diagram of workpiece with fixture

As this workpiece is symmetric in nature therefore we have created half of the work piece which will be automatically rotated in Fluent.

3.1.3.7 Parameter setting:

Properties of the work piece:

Material: Aluminium alloy

Composition: $Al - 95.8\%, Cr - 0.04\%, Cu - 0.15\%, Mg - 0.7\%$

Brinnel hardness no: 95

Ultimate tensile strength: $310MPa$

Yield strength: $276MPa$

Shear strength: $207MPa$

Media: polyborosiloxane + grease

Density = $1219kg/m^3$, viscosity = $789\ kg/pa - s$

Abrasive: silicon carbide

Diameter = $d_g = 15200/600 = 25.33\mu m$

3.1.3.8 Boundary conditions:

The schematic diagram of the computational domain of the half of the workpiece is shown in fig.

- At inlet a uniform velocity profile and at outlet a constant pressure is maintained with a fully developed flow condition.
- Along the wall a no slip boundary condition is applied.
- Along the axes of the cylindrical fixture, an axes symmetric boundary condition is applied.
- The inlet pressure is $35\ bar$.
- Volume fraction is 40%.

3.1.3.9 Numerical method:

To simplify the analysis following assumptions are made.

- The medium is homogenous
- The flow is quasistatic, incompressible and laminar

- The flow is axisymmetric
- There is no swirling motion of the fluid

To solve he continuity equation, momentum equation of the fluid flow along the constitutive viscosity model a commercial CFD package "FLUENT" (ANSYS 13) is used.

3.1.4.1 Steps of Fluent analysis:

Start the Fluent-import mesh file-setup-double precision

Problem set-up:

- Check the scale ,and convert them to mm by,

General-mesh-scale-specify scaling factor (0.001)

- Then check domain extent, volume statistics, face area statistic and mesh.
- Taking, solver- type-pressure based-velocity formulation-absolute-time –steady-2D space-axisymmetric
- Models-multiphase-edit-mixture
- Materials-fluid-change/create-name-polyborosiloxane-density(1219kg/m^3)-viscosity(0.789 kg/ms)-change/create-fluid-change/ create-fluent database(silicon carbide)-copy
- Phases-polyborosiloxane(primary phase)-drag coefficient-schiller naumann
  Secondary phase-silicon carbide-granular-properties-diameter ($25.33\mu m$)
- Cell zone condition-phase –polyborosloxane-type-fluid-phase-silicon carbide-type solid
- Boundary condition-zone-inlet-phase-mixture-type-velocity inlet-edit-velocity magnitude($0.012m/s$)
  Outlet-type-pressure based-operating condition ($101325Pa$)
- Reference values-compute from-inlet-reference zone-fluid
- Solution method-scheme-pressure coupled SIMPLE-gradient-least square cell based-momentum-second order upwind-volume fraction-first order upwind transient formulation-first order implicit
- Solution control-under relaxation factors-pressure(0.3)-momentum(0.6)-volume fraction(0.40)
- Monitors-residual print plot-edit-convergence criterion –absolute

- Solution initialization method-standard-compute from all zone-reference frame-absolute-initial values-silicon carbide volume fraction (-0.40)-initialize
- Run calculation-time step sizes(0.001)-number of time steps(10000)-max iteration/time step(30)-reporting interval(1)
- Then calculate

The iterations are stopped when the scaled residuals of velocity and the continuity equation approached an assymptotic value.

3.1.5.1 Modelling of material removal

For modelling of material removal the following assumptions are taken.

- All the abrasive particles are assumed to be spherical in in shape.
- The average diameter of the abrasive particle d_g is calculated from the mesh size number Me

  $$dg = 15200/Me$$

  We have taken Me =600
- Each abrasive particle comprises of a single active cutting edge.
- The load acting on the abrasive particle is assumed to be constant.so same amount of indentation is created by each abrasive on the workpiece.

Mechanism of material removal:

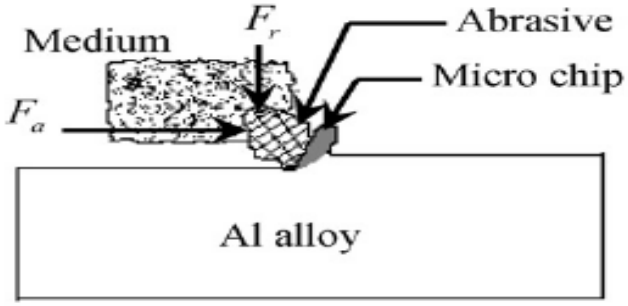

Figure No.14: Forces acting during AFM

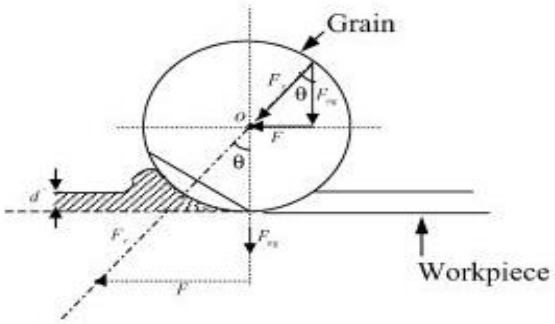

Figure No. 15: Mechanism of material removal

Jain et.al. Suggested that, when extrusion pressure is applied on the medium by the piston two types of forces are generated. I.e. radial or normal force and the axial force. Normal force is responsible for the indentation of the abrasive grain on the workpiece surface. And axial force is responsible for the material removal from the work piece surface. [1-6]

Normal force on a single grain:

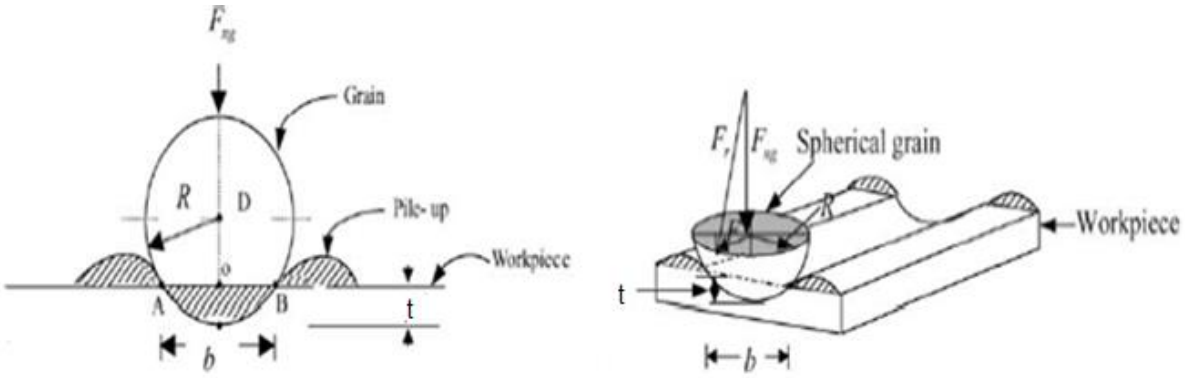

Figure No.16: Mechanism with forces during AFM

When the normal force F_n is applied on the workpiece during AFN it will indent to a depth t into the workpiece.

The normal force can be calculated as:

$$F_n = \sigma_{rad} \times A \qquad (5)$$

Where

$$A = \pi \times (d_g)^2 \qquad (6)$$

Where d_g the diameter of the abrasive particle. And is σ_{rad} is the radial stress acting on the work piece surface.

The indentation diameter d_i can be calculated as:

$$d_i = \sqrt{d_g}^{\,2} - \left(d_g - \frac{f_n \times 2 \times 10^{-6}}{9.81 \times H_{BHN}\, \pi d_g}\right)^2 \quad (7)$$

WhereH_{BHN} = Brinell hardness number of the workpiece material

= 99

The depth of indentation can be calculated as:

$$t = \frac{d_g}{2} - \frac{1}{2}\sqrt{d_g^2 - d_i^2} \quad (8)$$

During shearing of the workpiece surface the axial shear force F_a is acting, which must be greater than the reaction force on the abrasive particle by the workpiece material at the projected area.

The projected area can be calculated as:

$$A' = \frac{d_g^2}{4}\sin^{-1}\frac{2\sqrt{t(d_g - t)}}{d_g} - \sqrt{t(d_g - t)(\frac{d_g}{2} - t)} \quad (9)$$

The axial force can be calculated as:

$$F_a = (A - A') \times \tau_y \quad (10)$$

The reaction force can be calculated as:

$$F_R = A' \times \sigma_y \quad (11)$$

The volume of the material removal can be calculated as:

$$v_a = A' \times l_i \quad (12)$$

Where l_i is the contact length of grain on the with the work piece.

$$l_i = r \times \theta \quad (13)$$

Where θ is the contact angle of abrasive grain on the work piece.

θ Can be calculated as $$Cos\theta = d_i/r \quad (14)$$

3.2 Simulation on a cylindrical pipe:

Presently the CFD simulation of flow inside a pipe is also done.

Materials used:

Work piece: Al alloy

Yield strength=$276MPa$

Media: polyborosiloxane + grease

Density=$1219kg/m^3$, viscosity=789 $kg/m-s$

Abrasive particle: silicon carbide (diameter $25\mu m$)

Workpiece design: the work piece is designed by GAMBIT and the meshed.

Figure No. 17: The modelling and meshing of pipe

Diameter of the pipe: 5 mm no.

Length of pipe : 100 mm

3.2.1 Simulation through CFD (FLUENT: ANSYS 13):

In this study solid –liquid multi-phase flow mixture model is taken, with solver double precision and a low Reynolds number [31-36].

Boundary conditions:

Velocity inlet, pressure outlet, symmetrical centreline, Medium density is $1219\ kg/m^3$ and viscosity of $0.789\ pa-s$, Operating entrance pressure of $39bar$ and exit pressure is atmospheric.

Simulation: taking number iteration $= 1000$, Reporting interval = 1

Iterations are stopped when the residuals for the two component velocity and the continuity equation approached an asymptotic value.

Chapter 4

4.1 Result and discussion for Flat work-piece

In this study the simulation results of fluid flow analysis at different volume fraction and different extrusion pressure are discussed. Then calculation is made to find the various parameters like axial force, normal force, and volume of material removal by getting the results from the simulation.

4.1.1 Velocity distribution:

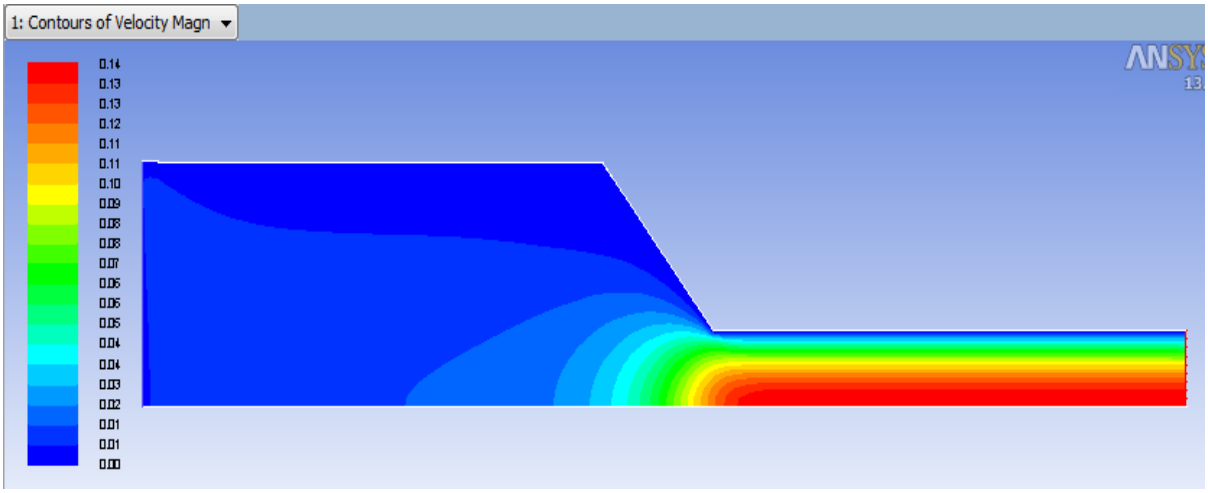

Figure No.18: Velocity distribution

From the figure we can conclude that the velocity changes when it reaches the taper exit, magnitude of velocity is maximum at the centre and decreases gradually towards the wall, because the effect of viscosity present in the media.

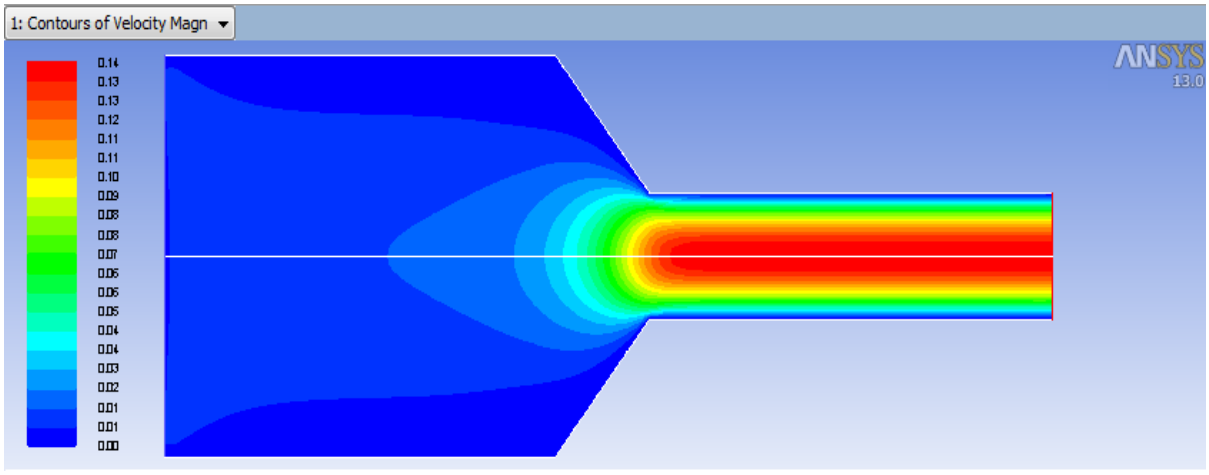

Figure No. 19: Velocity distribution on full view of work piece

4.1.2 Plot of velocity magnitude with position:

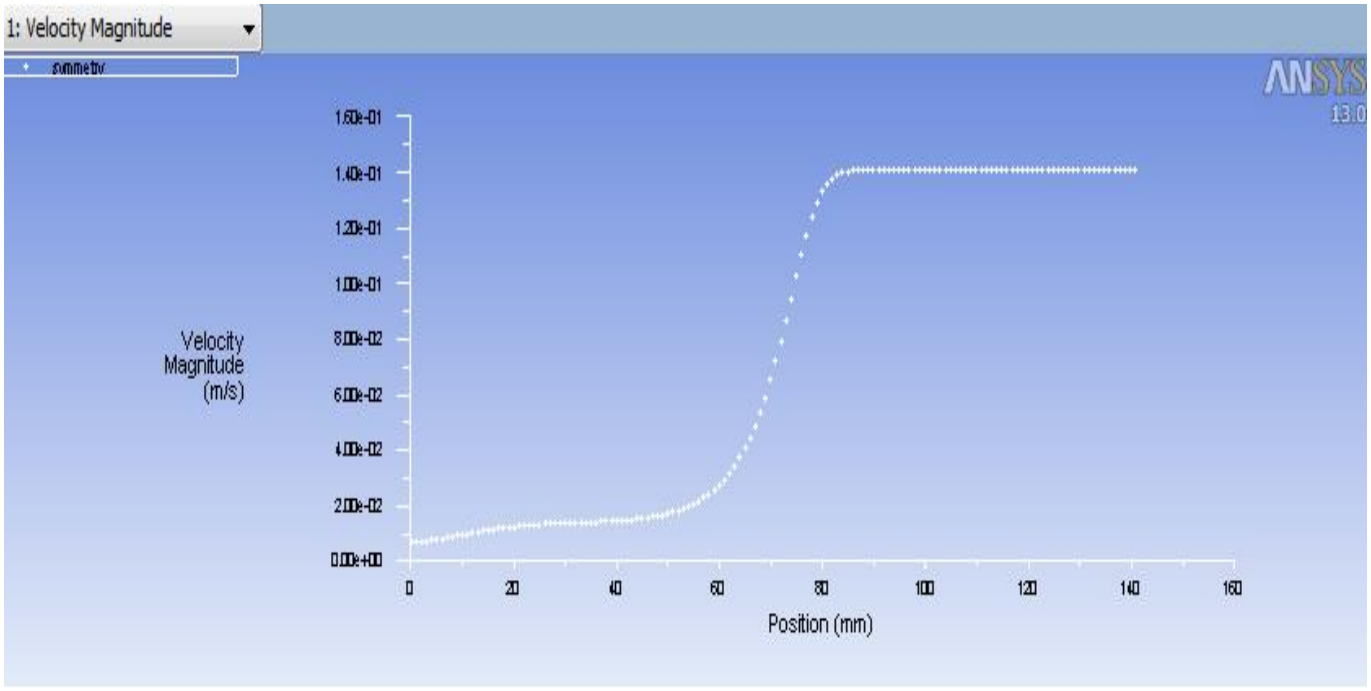

Figure No. 20: Velocity magnitude with position

From the plot of velocity we can determine that the velocity increases slowly up to the end of taper and then increases suddenly and then becomes constant.

4.1.3 Distribution of velocity vector:

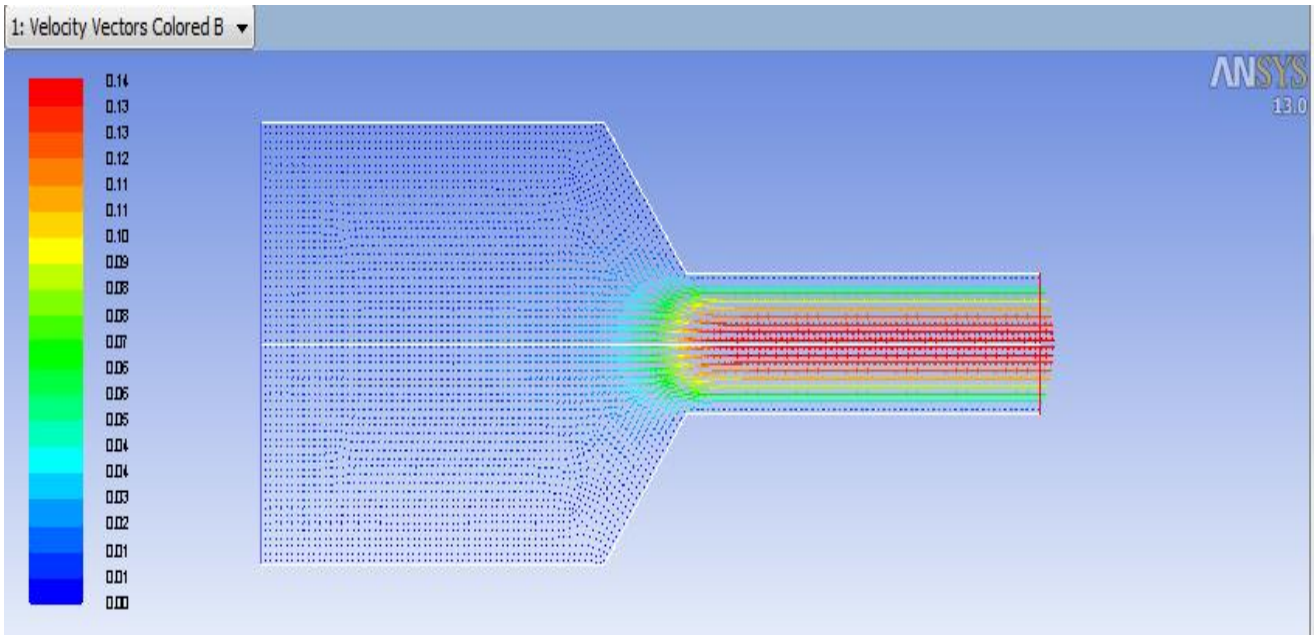

Figure No. 21: Distribution of velocity vector

4.1.4 Pressure distribution:

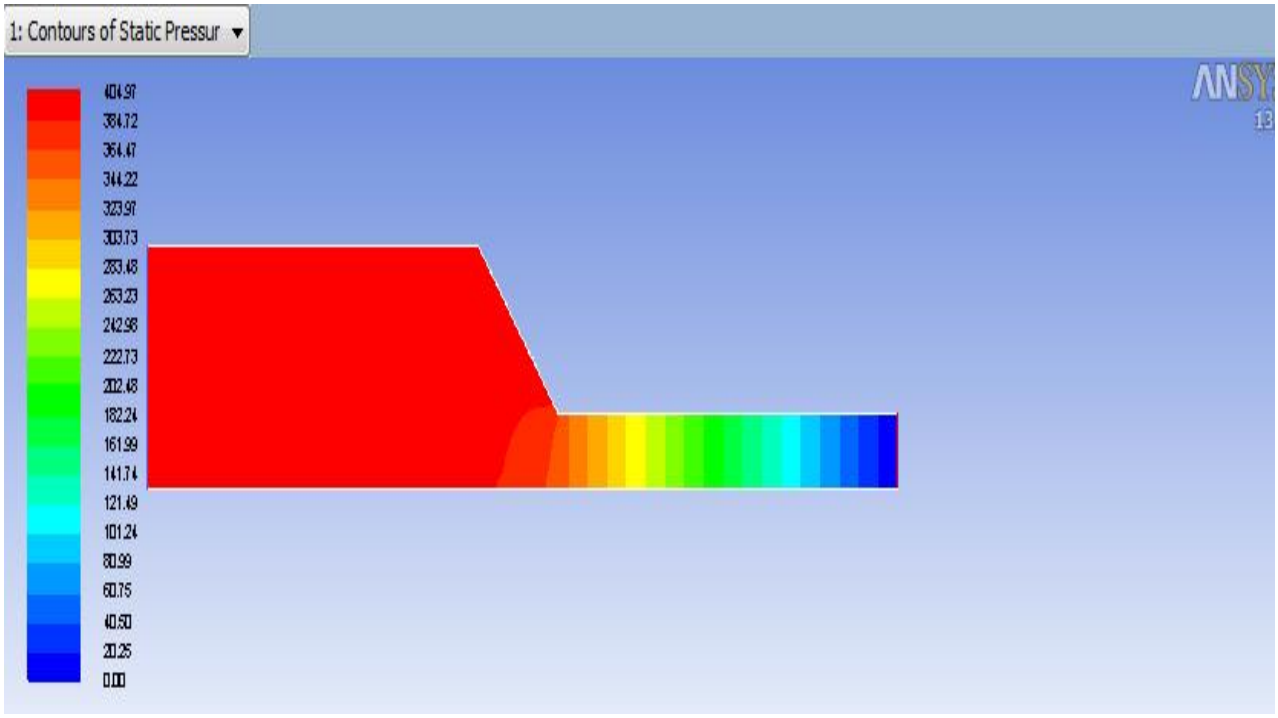

Figure No. 22: Pressure distribution

From the pressure distribution in the region of work piece fixture it remains constant upto the exit of the taper. After that it decreases gradually to the end of the workpiece.

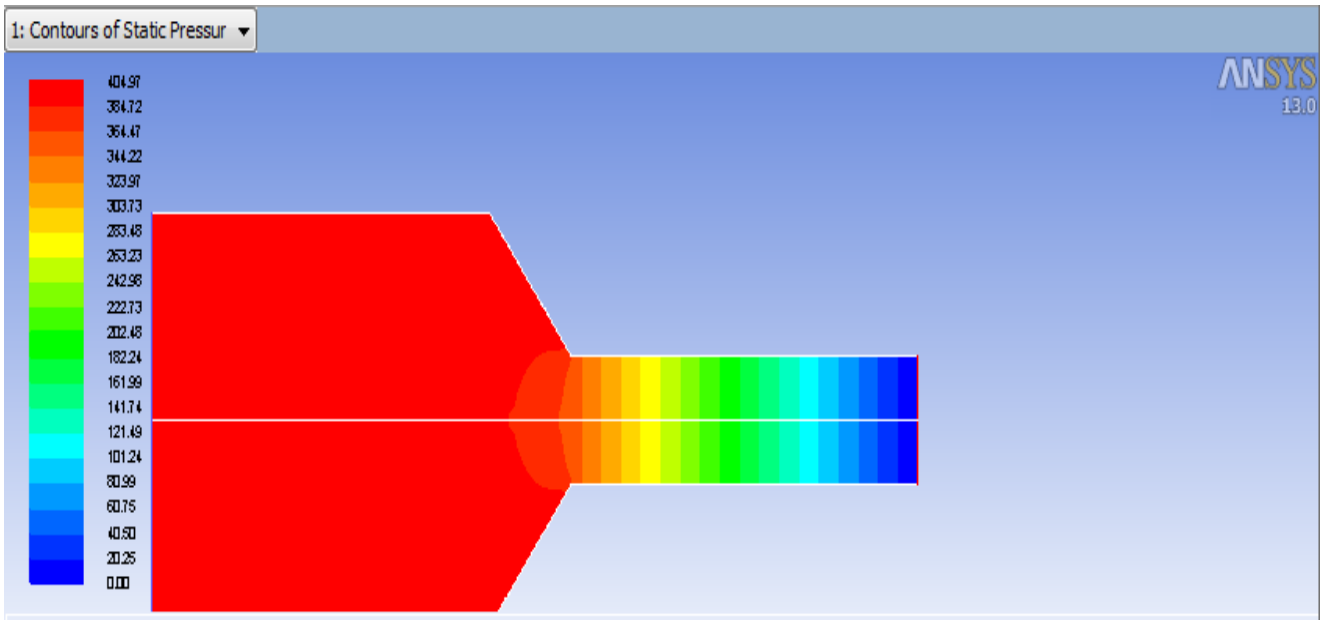

Figure No. 23: Pressure distribution of full view of work piece

4.1.5 Plot of static pressure with position:

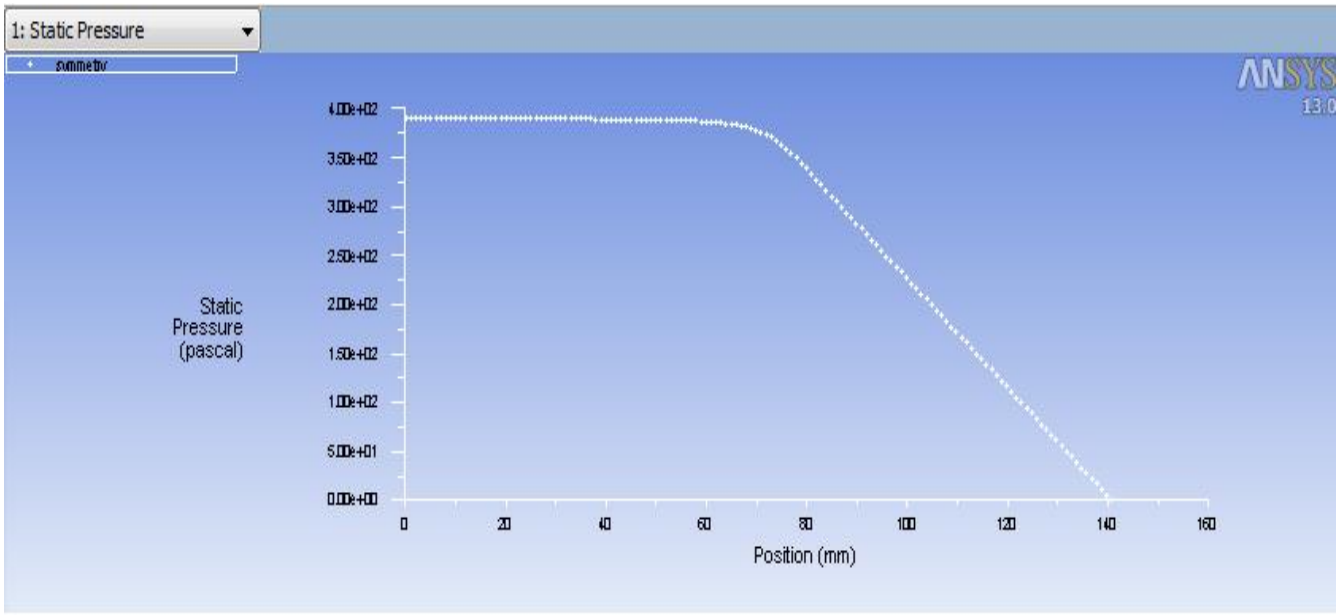

Figure No. 24: Static pressure with position

From the XY plot pressure distribution we conclude that initially the pressure is maximum at the inlet. It remains constant up to the taper then it starts decreasing gradually.

4.1.6 Strain distribution:

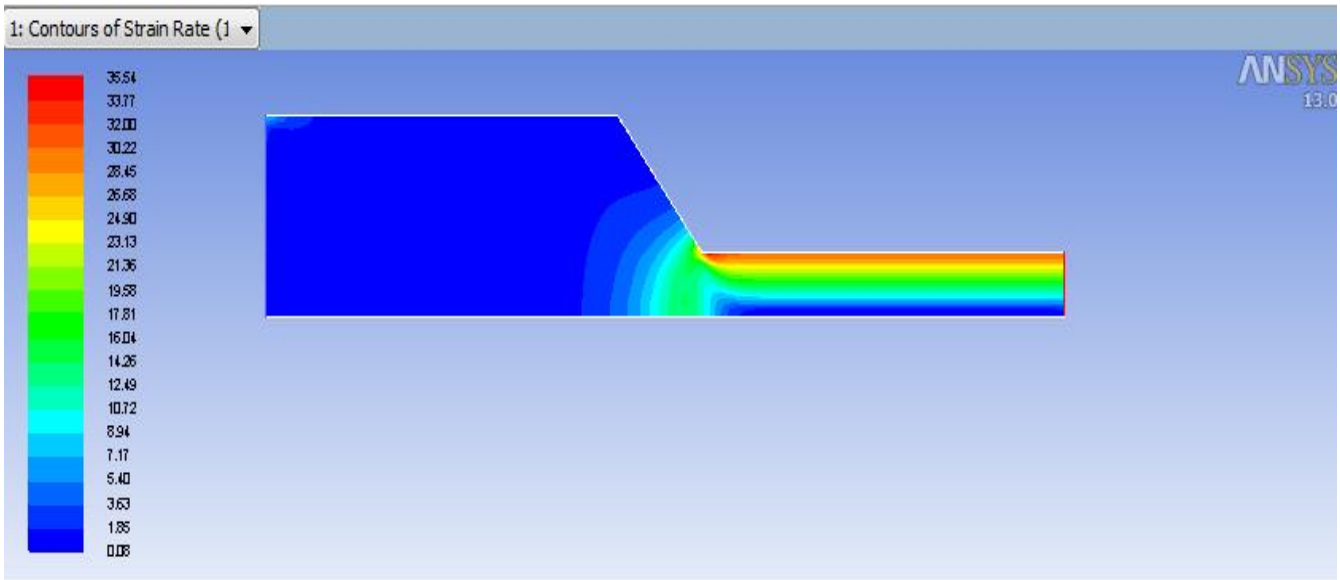

Figure No. 25: Strain distribution

From the figure above we can conclude that the strain is maximum at the wall. That's why stress will be produced there to remove the material.

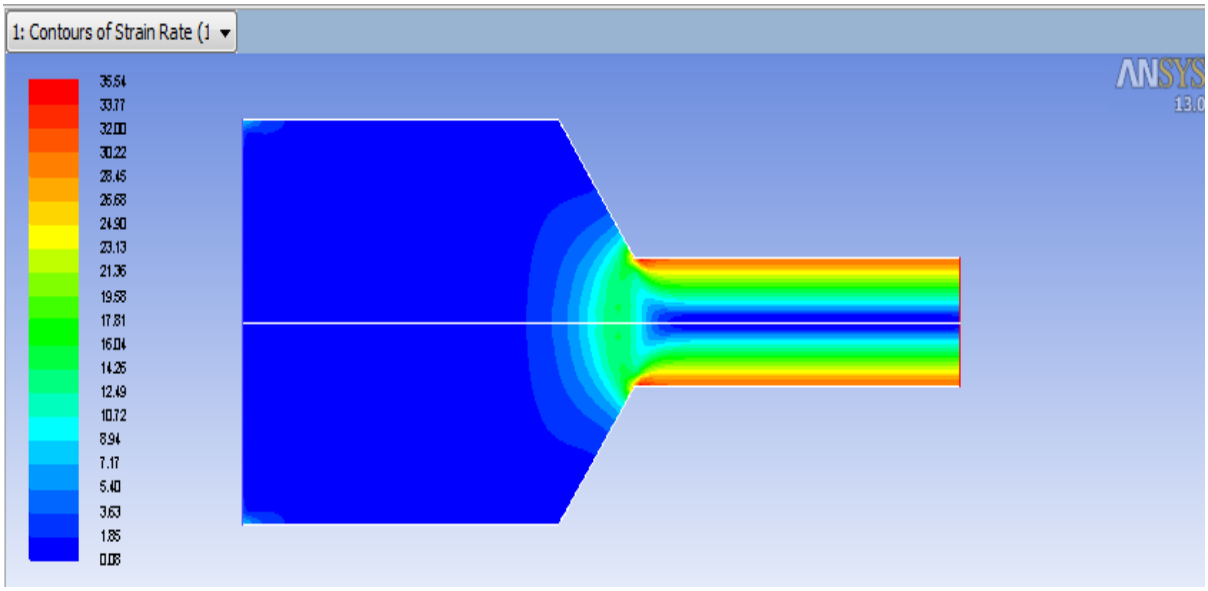

Figure No. 26: Strain distribution of full view of work piece.

4.1.7 Plot of strain rate with position:

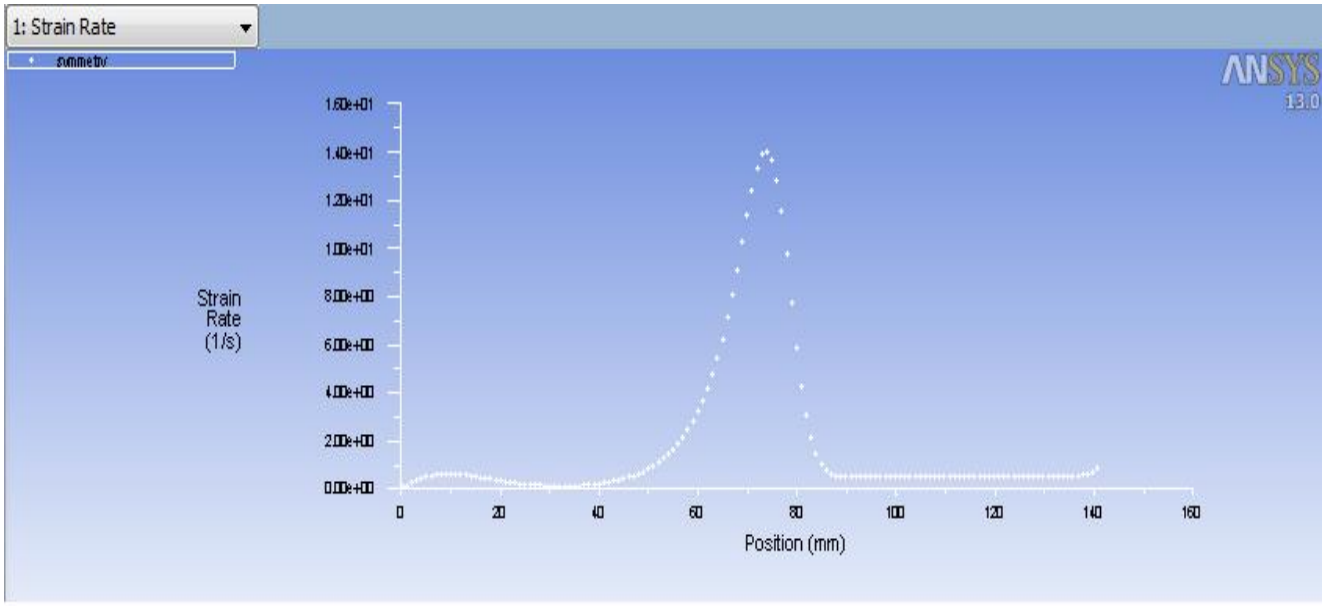

Figure No. 27: Strain rate with position

From the XY plot of strain distribution it is observed that, it is initially zero and then increases up to certain distance and then decreases up to distance 20 mm.Then it increases suddenly to its maximum value and then decreases and then becomes constant.

4.1.8 Plot of axial wall shear stress with position:

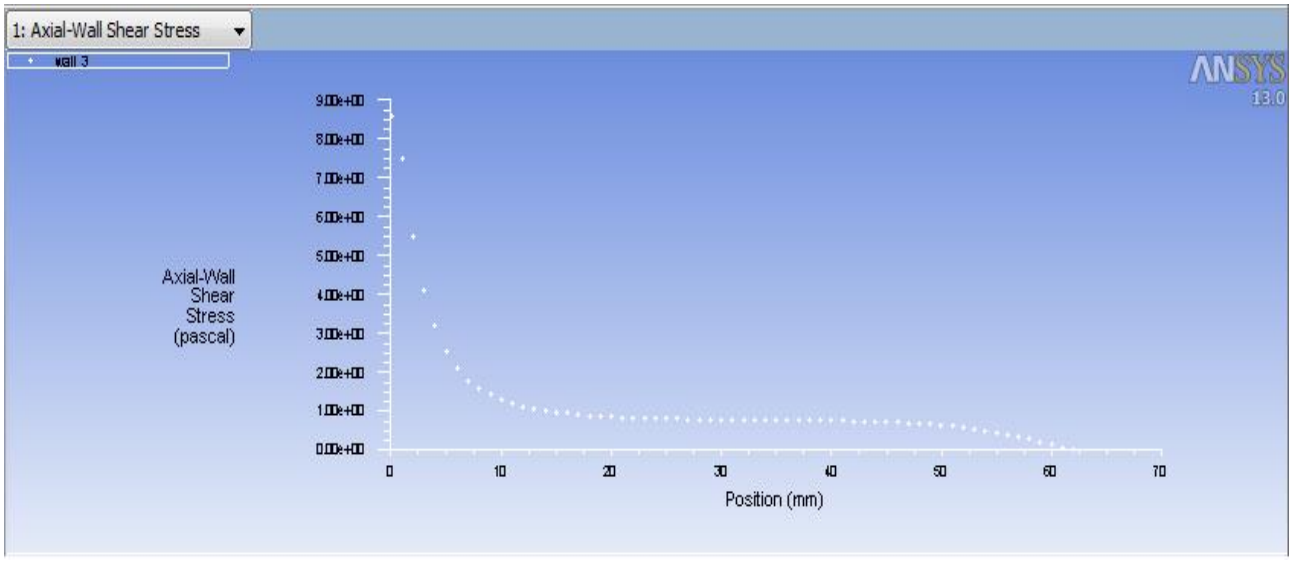

Figure No. 28: Axial wall shear stress with position

4.1.9 Plot of radial wall shear stress with position:

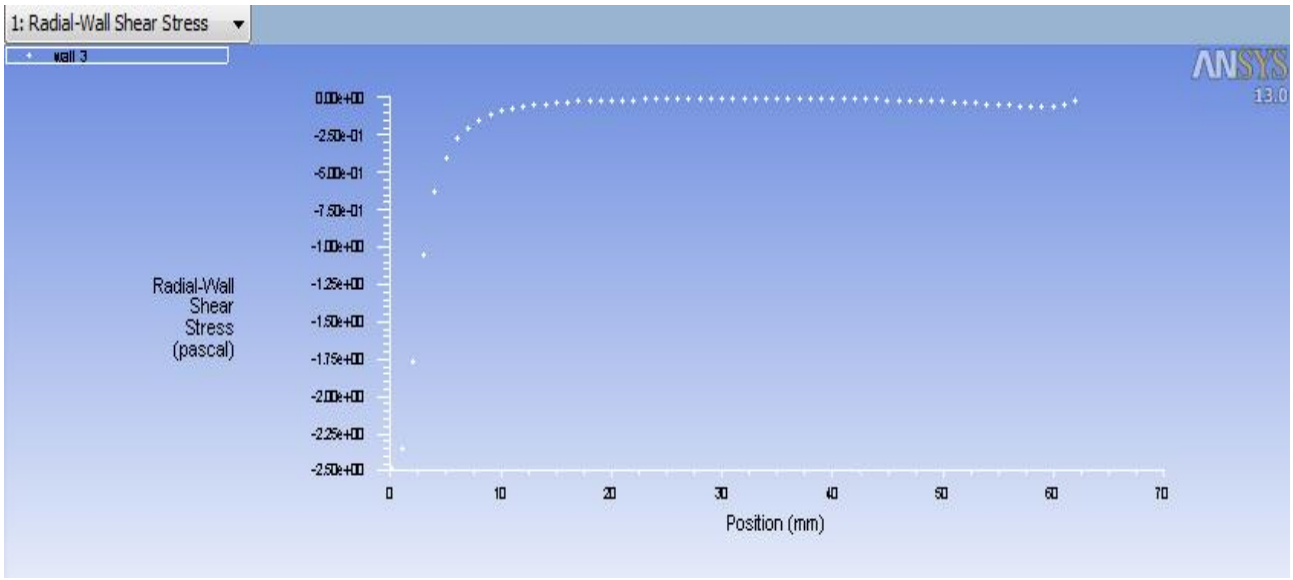

Figure No. 29: Radial wall shear stress with position

From CFD calculation the radial stress on the work piece material is,

$$\sigma_{rad} = 0.0690426\ Pa$$

Putting the value of radial stress on equation no. 5, we get normal force

$$F_n = 3.4748 \times 10^{-11}\ N$$

Now the indentation diameter can be calculated by putting the value of F_n in equation no. 7

$$d_i = 4.328*10^{-7} m$$

Putting the value of d_i in equation no 8. We get

Depth of indentation, $t = 1.07 \times 10^{-8}\ m$

Then projected area can be calculated as putting the value o $'t'$ in equation no. 9.

$A' = 3.70201 \times 10^{-10}\ m^2$

Now the reaction force can be calculated by putting the values in equation no.11

$F_r = 1.02175 \times 10^{-13}\ N$

From the CFD calculation the axial stress on the workpiece material is ,

$$\tau = 30.0356\ Pa$$

Now axial force can be calculated by putting the value of τ in equation no. 10

$$Fa = = 4.00644 \times 10^{-9}\ N$$

From the above calculation of axial force and reaction force we have found that the axial force is very much higher (10^4 times) than the reaction force. This signifies that the shearing action or the material removal from the work piece surface has been taken place.

Also from the equation no.14 we get,

$$2\theta = 176.09$$

Also we know $2\theta = Li/r$

So $Li = 1.2385 \times 10^{-5}\ m$

Now the volume of the material can be calculated from equation no. 12,

$$Va = A' \times l_i$$

$$= 4.75152 \times 10^{-15}\ m^3$$

4.2 Results and discussion of flow inside a pipe:

After the iteration is stopped the velocity and pressure distribution, the axial stress and the radial stresses are found as follows.

4.2.1 Velocity distribution:

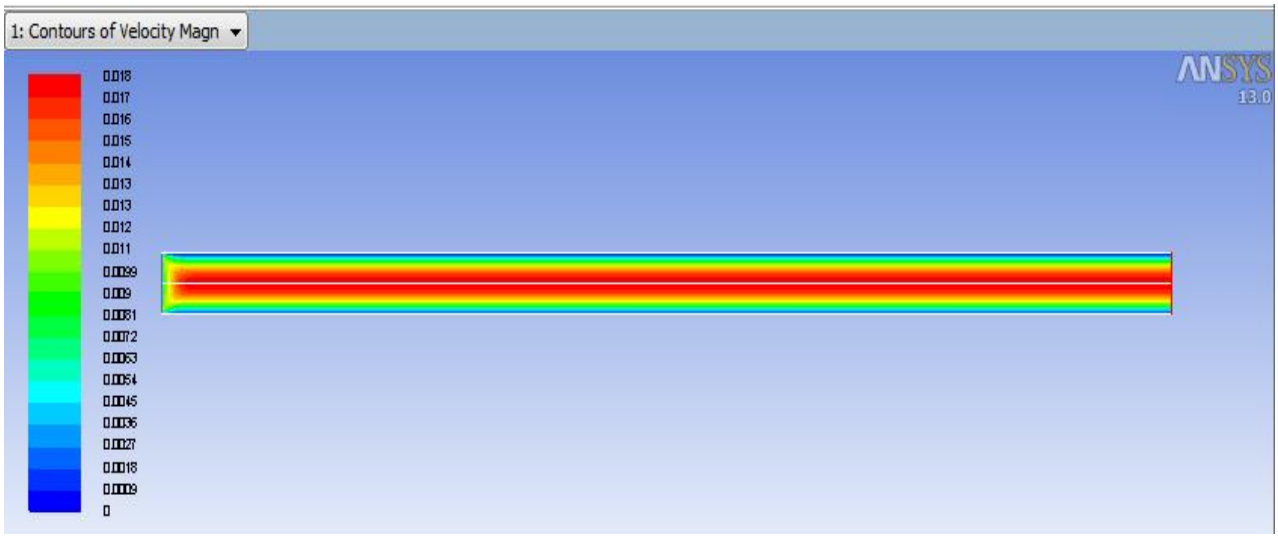

Figure No. 30: Velocity distribution

From the simulation of velocity it is found that the velocity is maximum at the centreline and is minimum at the wall.

4.2.2 Plot of velocity magnitude with position:

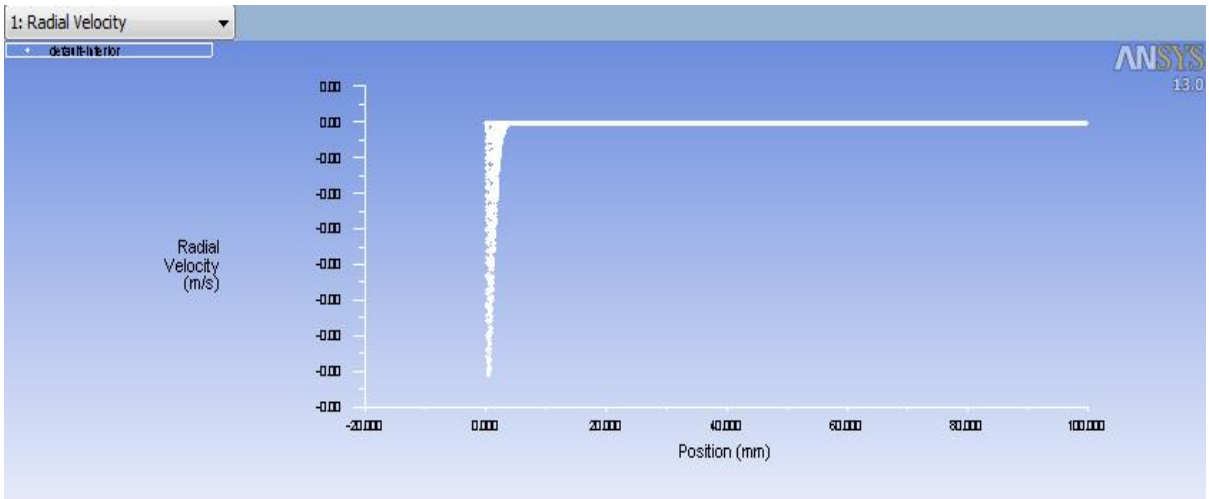

Figure No. 31: Velocity magnitude with in radial direction

4.2.3 Pressure distribution:

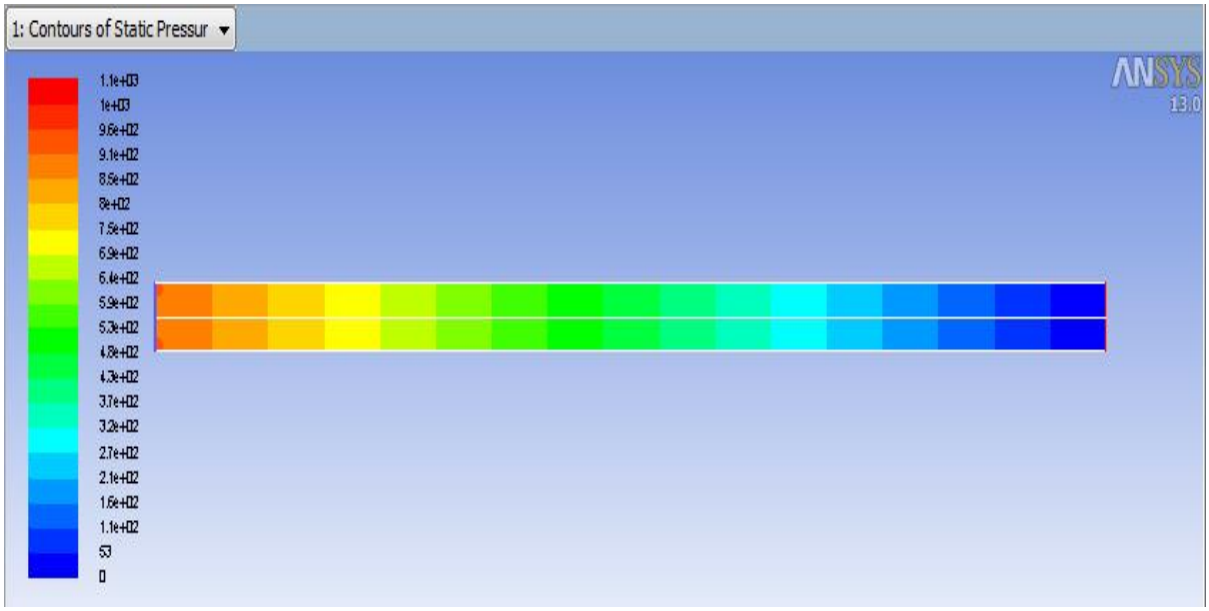

Figure No. 32: Pressure distribution

From the figure of pressure distribution it is found that the pressure decreases gradually from inlet to outlet.

4.2.4 Plot of Variation of pressure in axial direction:

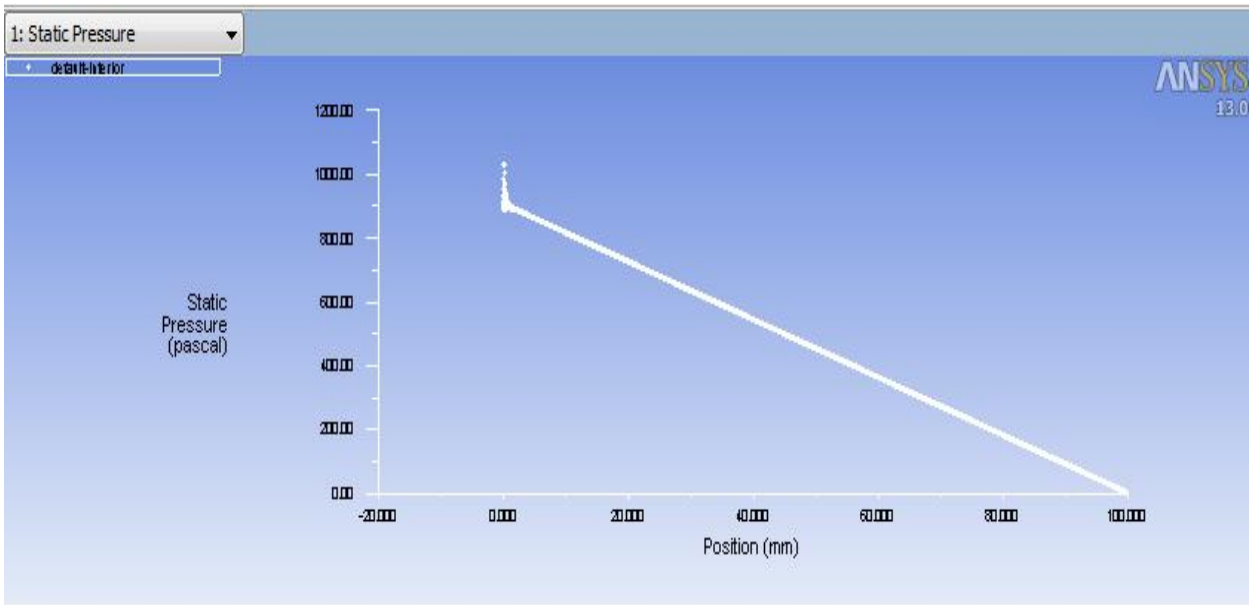

Figure No. 33: Static pressure with position

4.2.5 Plot of axial wall shear stress:

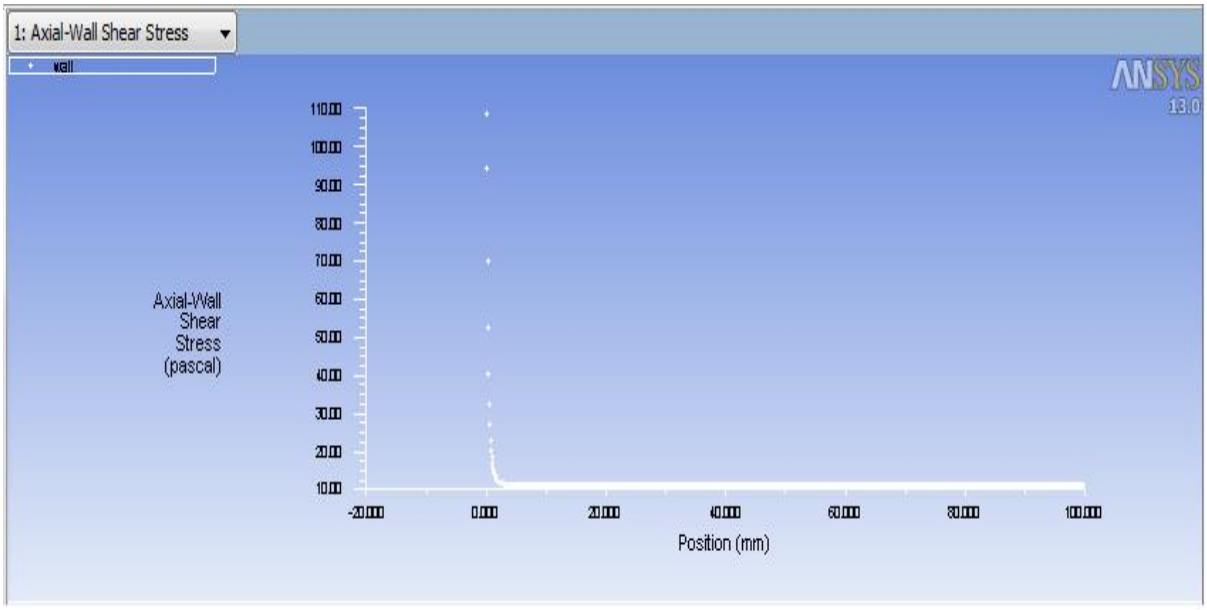

Figure No. 34: Axial wall shear stress with position

4.2.6 Plot of radial wall shear stress:

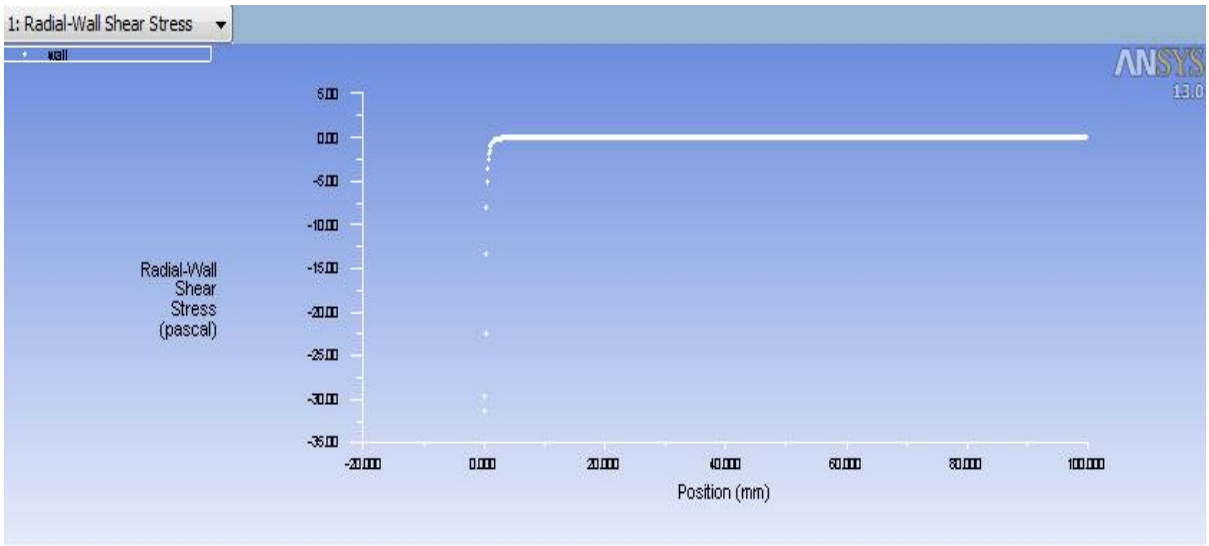

Figure No. 35: Radial wall shear stress with position

From CFD calculation the radial stress on the work piece material is,

$$\sigma_{rad} = 0.012195\ Pa$$

Putting the value of radial stress on equation no. 5 the normal force is found to be,

$$Fn = 6.1414 \times 10^{-12} N$$

Now the indentation diameter can be calculated by putting the value of Fn in equation no. 7

$$d_i = 4.187 \times 10^{-7} m$$

Putting the value of d_i in equation no.8 it is found that

Depth of indentation $t = 1.0098 \times 10^{-8}\ m$

Then projected area can be calculated as putting the value of $'t$ 'in equation no.9

$$A' = 3.4132 \times 10^{-10}\ m^2$$

Now the reaction force can be calculated by putting the values in equation no. 11

$$Fr = 1.02175 \times 10^{-13}\ \text{N}$$

From the CFD calculation the axial stress on the workpiece material is

$$\tau = 108.8988\ Pa$$

Now axial force can be calculated by putting the values in equation no. 10

$$Fa = 1.45248 \times 10^{-8} N$$

From the above calculation of axial force and reaction force we have found that the axial force is very much higher (10^5 times) than the reaction force.which signifies that the shearing action or the material removal from the work piece surface has been taken place.

Also from the equation no.14, θ can be calculated as:

$$2\theta = 176.03$$

So the contact length Li is

$$Li = r \times 2\theta = 1.2375 \times 10^{-6}$$

Now the volume of the material can be calculated by putting the values in equation no.12

$$Va = A' \times l_i$$

$$= 4.225 \times 10^{-16}\ m^3$$

Chapter 5

Optimization

Machinability of a material indicates towards adaptability to be manufactured by a machining process. In general, machinability can be defined as an optimal combination of factors such as low cutting force, high material removal rate, good surface integrity, accurate and consistent workpiece geometrical characteristics. There are various methods of optimization available. In this study we have used the Response surface methodology to optimize the work.

5.1 Response Surface Methodology:

Mainly response surface methodology (RSM) was carried out in this study. Usually, the correlation between the dependent variables and independent variables is either extremely complex. However, RSM gives a procedure which solves this problem [37, 39]. Assume that the decision maker is concerned with a system involving a dependent variable Y, which affects on the independent variable x_j. It is also taken that x_j is continuous and convenient. With RSM, the functional relationship between the output y and the levels of n input parameters can be written as:

$$y = f(x_1, x_2, x_3, \dots x_n) \quad (15)$$

A mathematical model for such a relationship does not necessarily exist. Thus, the first step in RSM is to get a suitable approximation for $f(x_1, x_2, x_3, \dots x_n)$ using a low-order polynomial in some section of the independent variables. If the approximated function has linear variables, a first-order polynomial can be used and written in terms of the independent variables:

$$y = f(x_1, x_2, x_3, \dots x_n) = a_0 + a_1 x_1 + a_2 x_2 + \cdots a_n x_n \quad (16)$$

Otherwise, a second-order polynomial can be used:

$$y = f(x_1, x_2, x_3, \dots x_n) = a_0 + \sum_{i=1}^{n} a_i\, x_i + \sum_{i=1}^{n} b_i\, {x_i}^2 + \sum_{i=1}^{n} \sum_{j=i-1}^{n-1} c_{ij} x_i x_j \quad (17)$$

The common use of second-order polynomial models is justified by the fact that they influence the nonlinear behavior of the system. Experimental designs for setting a second-order response surface must entail at least three levels of each variable so that the coefficients

in the model can be predictable. A rotation characteristic is required for response surface models because the orientation of the design, with respect to its surface, is unidentified. Hence, the orientation of the design is an important factor in regard to the response surface which affects the set of data and the fitting of the response surface. Here the DOE of three parameters with box-behnken design of 15 run conducted and that can be used for setting a second-order model to the response surface [37, 39]. This study used the Box–Behnken design because it allowed for fruitful estimation of the first-order and second-order coefficients. Using this experimental design, the levels of each parameter were assumed to be equally spaced. A least-squares method was used to approximate the coefficients to approximate the polynomials. The response surface analysis then proceeded in terms of the fitted surface. If the fitted surface is an enough estimation of the true functional relationship, then the analysis of the fitted response will be nearly correspondent to the analysis of the studied problem. Based on the RSM results, the design engineer can select the critical process controllable variables for reducing the variation in quality value significantly. The ultimate goal of RSM is to decide the optimal factor levels and to form the prediction function in the system. The MINITAB version 16 software was used to develop the experimental plan for RSM. The same software was also used to analyze the data collected by following the steps [39]:

1) Choose a transformation if desired. Otherwise, leave the option at “None”.

2) Select the suitable model to be used. The Fit Summary button shows the sequential F-tests, lack-of-fit tests and other adequacy measures that could be used to help in selecting the appropriate model.

3) Perform the analysis of variance (ANOVA) analysis of individual model coefficients and case information for analysis of residuals.

4) Inspect various diagnostic graphs to statistically validate to the model.

5) If the model looks good, generate model graphs, i.e. the contour and 3D graphs, for analysis. The study and inspection performed in steps (3) and (4) above will illustrate whether the model is good or otherwise. Very briefly, best model must be significant and the lack-of-fit must be insignificant.

5.1.1 Optimization techniques

Mathematical programming can represent one problem formulation that normalizes all deterministic operations research methodologies [39].The problem formulation is represented as:

Optimize $f(x_1, x_2, x_3, \dots x_n)$ (18)

Subject to $S_{lj} \leq x_j \leq S_{uj}$ (19)

$L_i \leq g_i(x_1, x_2, x_3, \dots x_n) \leq U_i$ (20)

Where j is 1, 2, 3 ... n, i is 1, 2, 3.... m.

In this study, $f(x_1, x_2, x_3, \dots x_n)$ was the concerned objective function with $x_1, x_2, x_3, \dots x_n$ as the controllable variable. x_j should fall between the mentioned low limit S_{lj} ,and the upper limit S_{uj}.The objective functions $g_i(x_1, x_2, x_3, \dots x_n)$ are less important than $f(x_1, x_2, x_3, \dots x_n)$. Thus, these objective functions are considered as constraints for multiple objective optimizations. For example, Eq. (4) is this type of constraint. The constraints should fall within the domain ofL_i & U_i.

5.1.2 Test for significance of the regression model

This test is performed as an ANOVA analysis by calculating the F-ratio, which is the ratio between the regression mean square and the mean square error. The F-ratio, also called the variance ratio, is the ratio of variance due to the effect of a variable and variance due to the error term. This ratio is used to calculate the significance of the model under investigation with respect to the variance of all the terms incorporated in the error term at the desired significance α-level. A significant model is preferred.

5.1.3 Test for significance on individual model coefficients

This test structures the basis for model optimization by adding or deleting coefficients through backward elimination, for-ward addition or stepwise elimination/addition/exchange. It engages the determination of the P-value or probability value, usually relating the risk of falsely refusing a given hypothesis. For example, a “Prob. Value > F” value on an F-test

informs the proportion of time you would anticipate to get the stated F-value if no factor effects are significant. The "Prob. Value > F" determined can be compared with the preferred probability or α-level. In general, the lowest order polynomial would be selected to adequately describe the system.

5.1.4 Test for lack-of-fit

As imitate measurements are available, a test indicating the consequence of the replicate error in comparison to the model dependent error can be performed. This test divides the residual or error sum of squares into two portions, one which is due to pure error which is based on the replicate measurements and the other due to lack-of-fit based on the model results. The test statistic for lack-of-fit is the ratio in between the lack-of-fit mean square and the pure error mean square. As previously, this F-test statistic can be used to find out as to whether the lack-of-fit error is significant or otherwise at the desired significance α-level. Insignificant lack-of-fit is desired as significant lack-of-fit designates that there might be contributions in the regression of response relationship that are not reported for by the model.

5.2 Results and discussions:

In this present study, the characteristic parameters of abrasive flow machining are taken of 3 variables and their domains are shown in Table no. 1 with high and low value. Here the Response Surface Methodology (RSM) is used for optimization of this operation. RSM is an efficient and fruitful method of optimization in statistical analysis. Design of Experiment (DOE) of above said three parameters with 15 runs is given in Table no. 2. The input variables of this machining are volumetric fraction, pressure and velocity which are tabulated in Table no. 3 with their standard and experimental run order. Then the out responses i.e. axial stress, radial stress and indentation depth are recorded in Table no. 4. For this optimization Minitab version 16 is utilized and gives 3D surface plots below.

Table No. 1: Value of Input Process Parameters

Process parameters	Unit	Code	Low	High
Volume fraction	%	A	40	50
Pressure	Bar	B	35	60
Velocity	m/sec	C	0.009	0.025

Table No. 2: Design Table Randomized

RUN	BLOCK	A	B	C
1	1	+	0	-
2	1	0	-	-
3	1	-	-	0
4	1	0	+	+
5	1	0	0	0
6	1	0	0	0
7	1	0	+	-
8	1	0	-	+
9	1	+	+	0
10	1	0	0	0
11	1	+	-	0
12	1	-	+	0
13	1	+	0	+
14	1	-	0	+
15	1	-	0	-

Table No. 3: Design table

Std. Order	Run Order	VOLUME FRACTION	PRESSURE	VELOCITY
6	1	50	47.5	0.009
9	2	45	35.0	0.009
1	3	40	35.0	0.017
12	4	45	60.0	0.025
15	5	45	47.5	0.017
14	6	45	47.5	0.017
10	7	45	60.0	0.009
11	8	45	35.0	0.025
4	9	50	60.0	0.017
13	10	45	47.5	0.017
2	11	50	35.0	0.017
3	12	40	60.0	0.017
8	13	50	47.5	0.025
7	14	40	47.5	0.025
5	15	40	47.5	0.009

Table No. 4: Value of Output responses

Run Order	AXIAL STRESS	RADIAL STRESS	INDENTATION DEPTH
1	41.064	0.236	1.340
2	30.142	0.092	1.080
3	30.052	0.069	1.070
4	46.987	0.286	1.876
5	40.764	0.219	1.241
6	40.981	0.221	1.253
7	45.894	0.275	1.864
8	30.239	0.108	1.092
9	47.234	0.296	1.982
10	40.542	0.241	1.261
11	30.438	0.139	1.116
12	45.564	0.261	1.881
13	40.763	0.209	1.219
14	40.439	0.275	1.283
15	40.018	0.237	1.249

Axial stress:

The regression analysis is carried out for the given output responses. First the regression table axial stress is shown in Table no. 5 in which pressure, the square term of pressure and the interaction between volume fraction and pressure have significant value as their values are less than p=0.05. Here R-square value comes 99.94 % which is acceptable. Then Analysis of Variance (ANOVA) analysis for axial stress has been done in Table no. 6 in which the total degree of freedom of input parameters is 14.

Table No. 5: Estimated Regression Coefficients for AXIAL STRESS

TERM	COEFFICIENT	SE COEFFICIENT	T	P
CONSTANT	-26.52	11.77	-2.254	0.074
VOLUME FRACTION	0.25	0.47	0.530	0.619
PRESSURE	1.80	0.12	15.017	0.000
VELOCITY	157.81	165.33	0.954	0.384
VOL.FRACTION*VOL.FRACTION	-0.00	0.01	0.721	0.503
PRESSURE*PRESSURE	-0.02	0.00	-18.330	0.000
VELOCITY*VELOCITY	-1545.57	2001.44	-0.772	0.475
VOL.FRACTION*PRESSURE	0.01	0.00	2.608	0.408
VOL.FRACTION*VELOCITY	-4.51	3.08	-1.467	0.202
PRESSURE*VELOCITY	2.49	1.23	2.023	0.099

S = 0.246134 PRESS = 3.52154

R-Sq. = 99.94%, R-Sq. (pred) = 99.36%, R-Sq. (adj) = 99.85%

Table No. 6: Analysis of Variance for AXIAL STRESS:

SOURCE	DF	SEQ SS	Adj SS	Adj MS	F
REGRESSION	9	547.887	547.887	60.8763	1004.86
LINEAR	3	526.691	14.020	4.6734	77.14
VOL.FRACTION	1	1.467	0.017	0.0170	0.28
PRESSURE	1	525.010	13.661	13.6610	225.50
VELOCITY	1	0.215	0.055	0.0552	0.91
SQUARE	3	20.405	20.405	6.8016	112.27
VOL.FRACTION*VOLFRACTION	1	0.025	0.032	0.0315	0.52
PRESSURE*PRRESSURE	1	20.343	20.335	20.3546	335.99
VELOCITY*VELOCITY	1	0.036	0.036	0.0361	0.60
INTERACTION	3	0.790	0.790	0.2635	4.35
VOL.FRACTION*PRESSURE	1	0.412	0.412	0.4122	6.80
VOL.FRACTION*VELOCITY	1	0.130	0.130	0.1303	2.15
PRESSURE*VELOCITY	1	0.248	0.248	0.2480	4.09
RESIDUAL ERROR	5	0.303	0.303	0.0606	-
LACK OF FIT	3	0.207	0.207	0.0688	1.43
PURE ERROR	2	0.096	0.096	0.0482	-
TOTAL	14				

The first order quadratic equation is generated which is given below:

$$\text{AXIAL STRESS} = 4.42000 + 0.08570^{*} A + 0.64800^{*}B + 20.50000^{*}C \quad (21)$$

Radial stress:

The regression analysis for radial stress is shown in table no 8.In which the pressure, the square term of pressure have significant value as their values are less than 0.05. Here R-sq value comes 94.46% which is acceptable. The analysis of variance for radial stress has been done in table no.9 in which total degree of freedom of input parameters are 14.

Table No.7: Estimated Regression Coefficients for RADIAL STRESS

TERM	COEF.	SE COEF.	T	P
CONSTANT	-0.8331	1.360	-0.613	0.567
VOL.FRACTION	-0.0093	0.055	-0.171	0.871
PRESSURE	0.0394	0.014	2.840	0.036
VELOCITY	16.4805	19.013	0.863	0.428
VOL.FRACTION*VOL.FRACTION	0.0003	0.001	0.448	0.673
PRRESSURRE*PRESSURE	-0.003	0.000	-2.863	0.035
VELOCITY*VELOCITY	87.8906	231.255	0.380	0.720
VOL.FRACTION*PRESSURE	-0.0001	0.000	-0.615	0.565
VOL.FRACTION*VELOCITY	-0.4062	0.350	-1.143	0.305
PRESSURE*VELOCITY	-0.0125	0.0142	-0.088	0.933

S = 0.0284394 PRESS = 0.060634

R-Sq = 94.68%, R-Sq (pred) = 20.25% R-Sq (adj) = 85.11%

Table No. 8: Analysis of Variance for RADIAL STRESS

SOURCE	DF	Seq SS	Adj SS	AdJ MS	F
REGRESSION	9	0.071985	0.071985	0.007998	9.89
LINER	3	0.063373	0.007376	0.002459	3.04
VOL.FRACTION	1	0.000180	0.000024	0.000024	0.03
PRESSURE	1	0.063012	0.006522	0.006522	8.06
VELOCITY	1	0.000180	0.000602	0.000602	0.74
SQUARE	3	0.007243	0.007243	0.002414	2.98
VOL.FRACTION*VOL.FRACTION	1	0.000319	0.000162	0.000162	0.20
VOL.FRACTION*PRESSURE	1	0.006806	0.006630	0.006630	8,20
PRESSURE*VELOCITY	1	0.000117	0.000117	0.000117	0.14
INTERACTION	3	0.001369	0.001369	0.000456	0.56
VOL.FRACTION*PRESSURE	1	0.000306	0.000306	0.000306	0.38
VOL.FRACTION*VELOCITY	1	0.001056	0.001056	0.001056	1.31
PRESSURE*VELOCITY	1	0.000006	0.000006	0.000006	0.01
RESIDUAL ERROR	5	0.004044	0.004044	0.000809	-
LACK OF FIT	3	0.003748	0.003748	0.001249	8.44
PURE ERROR	2	0.000296	0.000296	0.111148	-
TOTAL	14				

The first order quadratic equation is generated which is given below.

RADIAL STRESS = - 0.17900 + 0.00095*A + 0.00710*B + 0.59000*C (22)

Depth of indentation:

The regression analysis of depth of indentation is shown in table no.9.in which the pressure and the square term of pressure have significant value as their values are less than 0.05.Here R-sq value comes as 99.67% which is acceptable. The analysis of variance for depth of indentation has been done in table no .10, in which total no. of degree of freedom of input parameters are 14.

Table No. 9: Estimated Regression Coefficients for INDENTATION DEPTH

TERM	COEFF.	SE COEFF	T	P
CONSTANT	4.835	1.516	3.189	0.024
VOL.FRACTION	-0.089	0.061	-1.462	0.204
PRESSURE	-0.119	0.015	-7.700	0.001
VELOCITY	46.107	21.301	2.165	0.083
VOL.FRACTION*VOLFRACTION	0.001	0.001	1.676	0.154
PRESSURRE*PRESSURE	0.001	0.000	14.144	0.000
VELOCITY*VELOCITY	-102.865	157.858	-0.399	0.706
VOL.FRACTION*PRRESSURE	0.000	0.000	8.867	0.425
VOL.FRACTION*VELOCITY	-0.969	0.396	-2.444	0.058
PRESSURE*VELOCITY	0.000	0.159	0.000	1.000

S = 0.0317109 PRESS = 0.07766

R-Sq = 99.67%, R-Sq (pred) = 94.94%, R-Sq (adj) = 99.08%

Table No. 10: Analysis of Variance for INDENTATION DEPTH

SOURCE	DF	Seq SS	Adj SS	Adj MS	F
REGRESSION	9	1.53033	1.53033	0.170036	169.09
LINER	3	1.32053	0.0673	0.022542	22.42
VOL.FRACTION	1	0.00378	0.00215	0.002149	2.14
PRESSURE	1	1.31625	0.05963	0.59628	59.30
VELOCITY	1	0.00050	0.00471	0.004711	4.69
SQUARE	3	0.20303	0.20303	0.067677	67.30
VOL.FRACTION*VOL.FRACTION	1	0.00049	0.00283	0.002826	2.81
PRESSURE*PRESSURE	1	0.20238	0.20031	0.200308	199.20
VELOCITY*VELOCITY	1	0.00016	0.00016	0.000160	0.16
INTERACTION	3	0.00676	0.00676	0.002254	2,24
VOL.FRACTION*PRESSURE	1	0.00076	0.00076	0.000756	0.75
VOL.FRACTUION*VELOCITY	1	0.00601	0.00601	0.006006	5.97
PRESSURE*VELOCITY	1	0.00000	0.00000	0.000000	0.00
RESIDUAL ERROR	5	0.00503	0.00503	0.001006	-
LACK OF FIT	3	0.00483	0.00483	0.001608	15.87
PURE ERROR	2	0.00020	0.00101	0.000101	-
TOTAL	14				

The first order quadratic equation is generated which is given below.

INDENTATION DEPTH = - 0.33300 + 0.00435*A+ 0.03250*B - 0.98000*C (23)

5.2.1 Residual plots:

Axial stress:

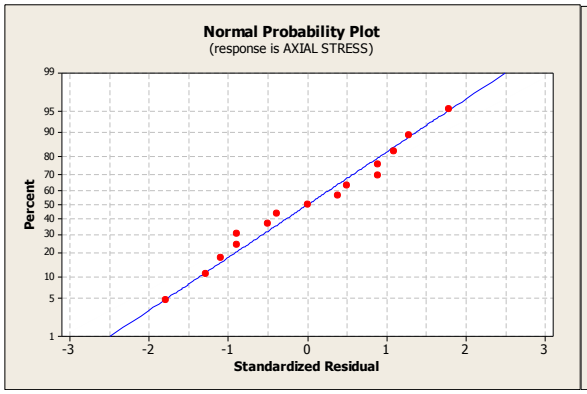

Figure. No. 36

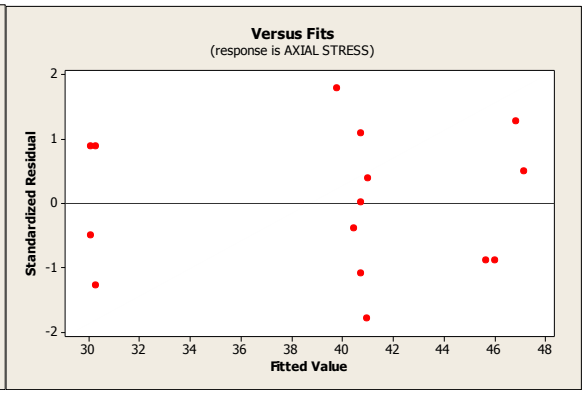

Figure. No. 37

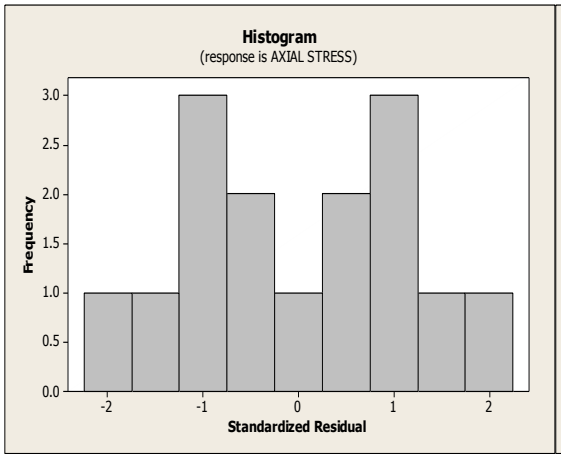

Figure No. 38

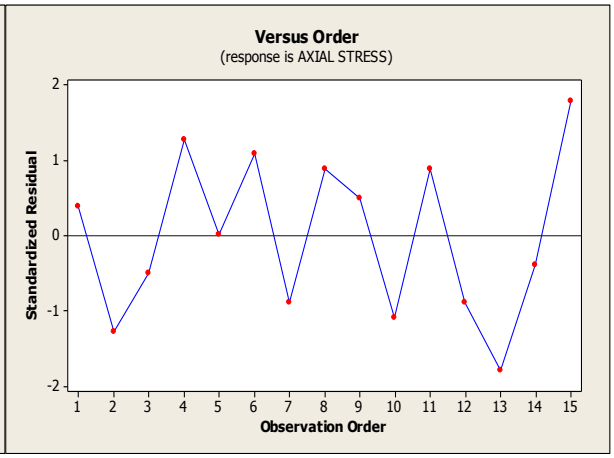

Figure No.39

The normal probability plot of output response of axial stress is plotted in Fig. no. 36 in which almost all the points are situated on the straight line. Thus, the results which are obtained for axial stress are correct. Then fitted value vs. standardized residual value plot is given in Fig. no. 37. In this graph no pattern of these points is formed. So, the input parameters are fitted well in 95 % confidence interval. The histogram plot of axial stress is shown in Fig. no. 38 in which all the columns are formed into normal probability distribution. Therefore, the present result indicates the realistic analysis of abrasive flow machining which is carried out in a successful manner. The plot between standardized order and residual values is presented in Fig. no. 39 where minimum axial stress is occurred in the 13^{th} run and similarly at the 15^{th} run the maximum value is obtained.

Radial stress:

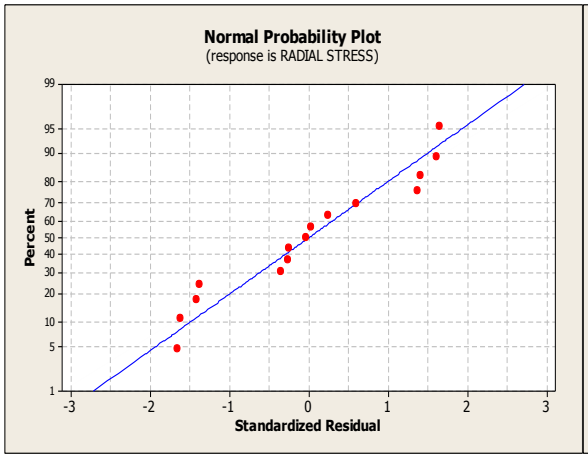

Figure No.40:

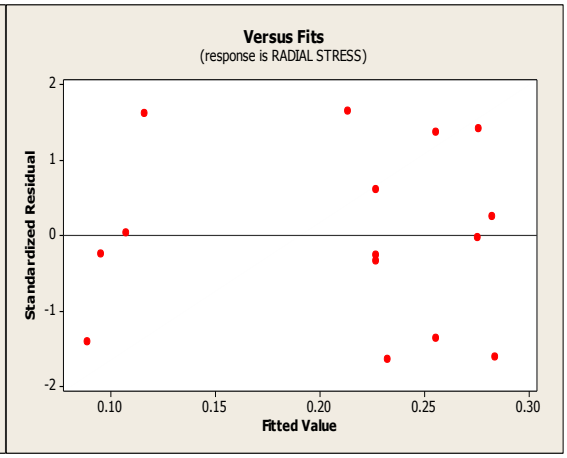

Figure No. 41:

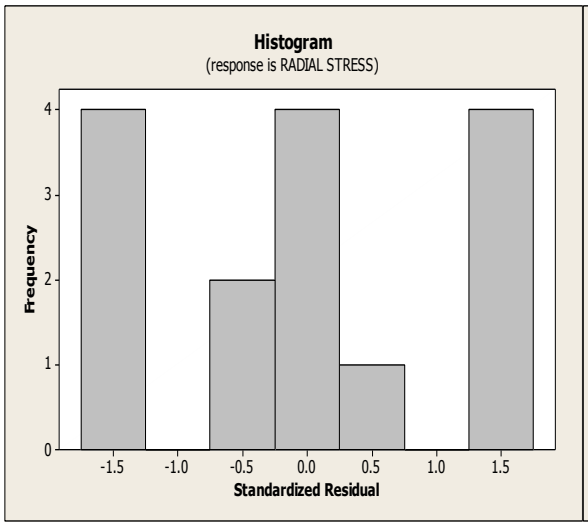

Figure No. 42:

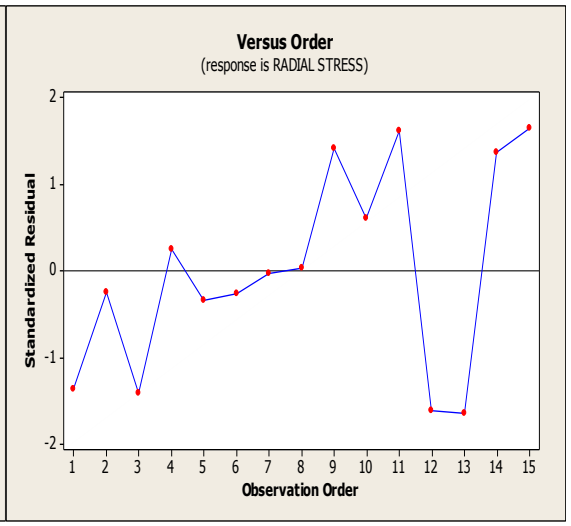

Figure No. 43:

The normal probability plot of output response of radial stress is plotted in Fig. no. 40 in which almost all the points are situated on the straight line. Thus, the results which are obtained for radial stress are correct. Then fitted value vs. standardized residual value plot is given in Fig. no. 41. In this graph no pattern of these points is formed. So, the input parameters are fitted well in 95 % confidence interval. The histogram plot of radial stress is shown in Fig. no. 42 in which all the columns are formed into normal probability distribution. Therefore, the present result indicates the realistic analysis of abrasive flow machining which is carried out in a successful manner. The plot between standardized order and residual values is presented in Fig. no. 43 where minimum radial stress is occurred in the 13^{th} run and similarly at the 11^{th} run the maximum value is obtained.

Indentation depth:

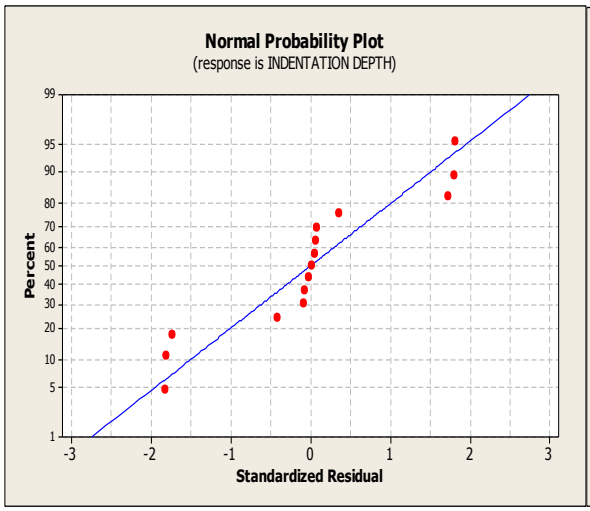

Figure No. 44:

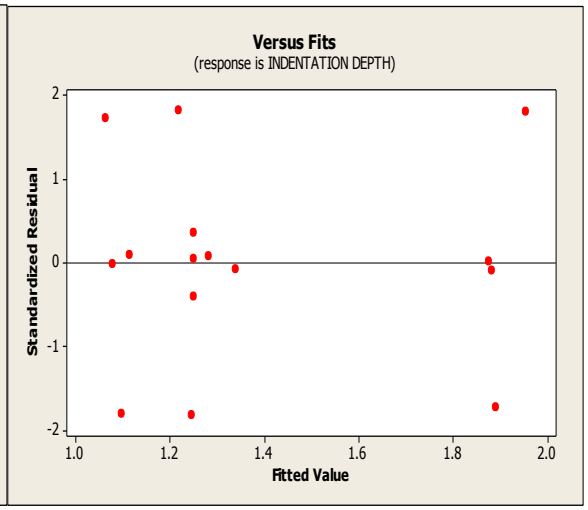

Figure No. 45:

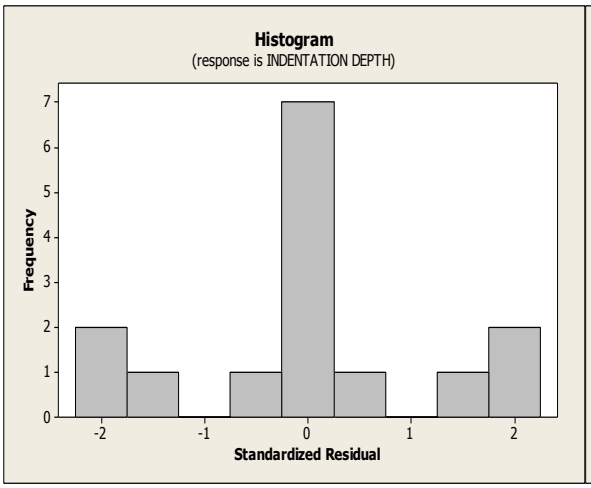

Figure No. 46

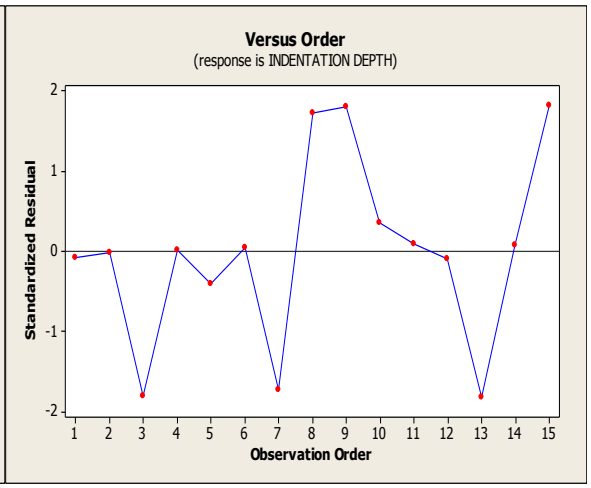

Figure No. 47

The normal probability plot of output response of indentation depth is plotted in Fig. no. 44 in which almost all the points are situated on the straight line. Thus, the results which are obtained for indentation depth are correct. Then fitted value vs. standardized residual value plot is given in Fig. no. 45. In this graph no pattern of these points is formed. So, the input parameters are fitted well in 95 % confidence interval. The histogram plot of indentation depth is shown in Fig. no. 46 in which all the columns are formed into normal probability distribution. Therefore, the present result indicates the realistic analysis of abrasive flow machining which is carried out in a successful manner. The plot between standardized order and residual values is presented in Fig. no. 47 where minimum indentation depth is occurred in the 13^{th} run and similarly at the 9^{th} run the maximum value is obtained.

5.2.2 Contour plots:

Axial stress:

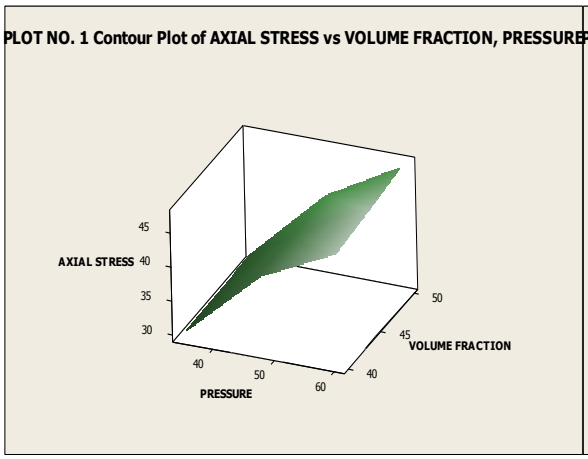

Figure No. 48

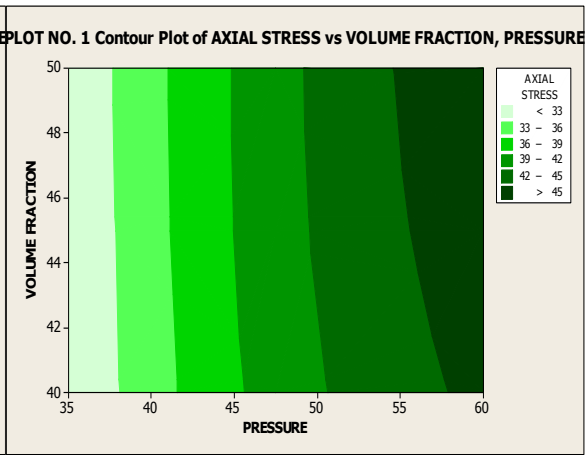

Figure No. 49

The 3D contour plot of axial stress vs. interaction of volume fraction and pressure is presented in Fig. no. 48 which show the plot increases with both increasing in pressure and volume fraction respectively. The 2D contour plot of axial stress vs. interaction of volume fraction and pressure is shown in Fig. no. 49.

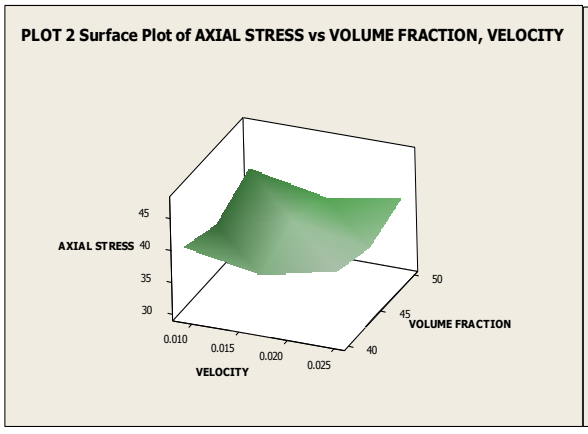

Figure No. 50

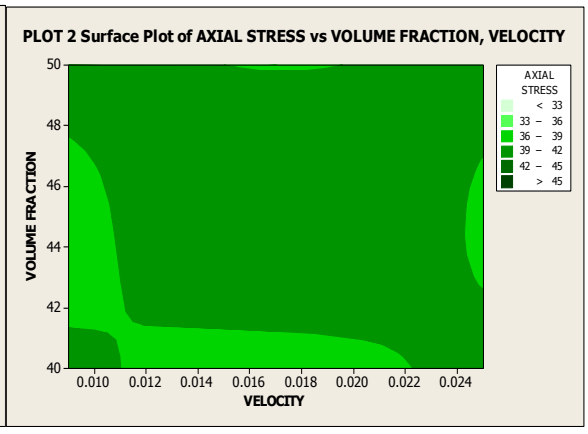

Figure No. 51

The 3D contour plot of axial stress vs. interaction of volume fraction and velocity is presented in Fig. no. 50 which show the plot increases at the middle region of velocity and volume fraction. The 2D contour plot of axial stress vs. interaction of volume fraction and velocity is shown in Fig. no. 51.

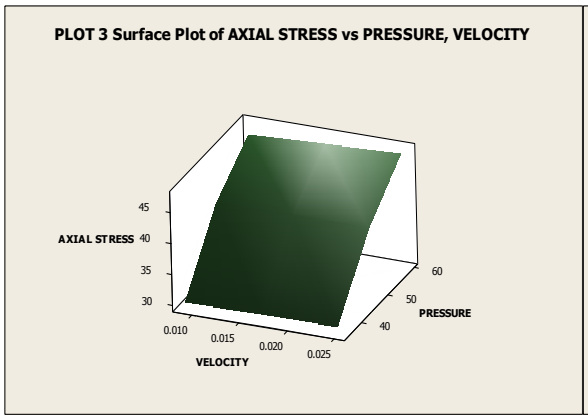

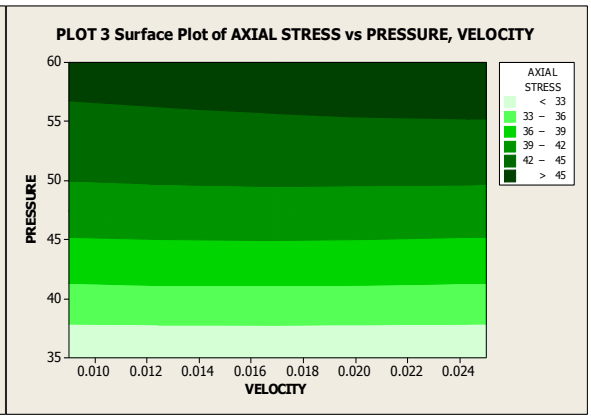

Figure No. 52 Figure No. 53

The 3D contour plot of axial stress vs. interaction of velocity and pressure is presented in Fig. no. 52 which show the plot increases with increasing by pressure and remains constant with velocity. The 2D contour plot of axial stress vs. interaction of velocity and pressure is shown in Fig. no. 53.

Radial stress:

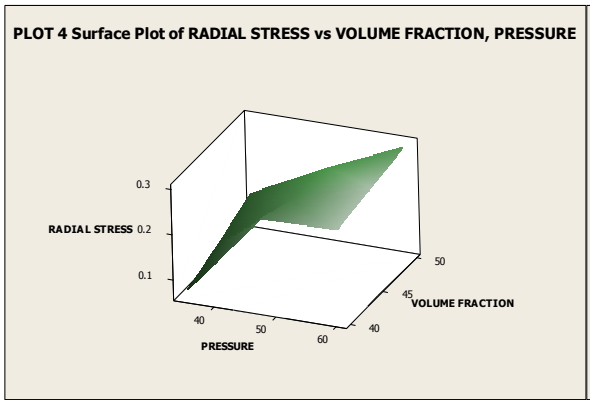

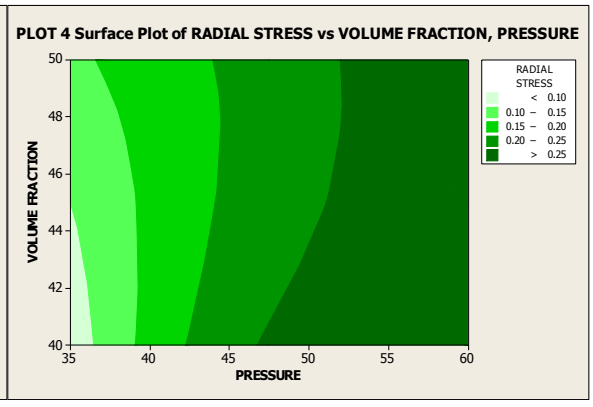

Figure No. 54 Figure No. 55

The 3D contour plot of radial stress vs. interaction of volume fraction and pressure is presented in Fig. no. 54 which show the plot increases with increasing in pressure in high manner and in case of volume fraction it increases slowly. The 2D contour plot of radial stress vs. interaction of volume fraction and pressure is shown in Fig. no. 55.

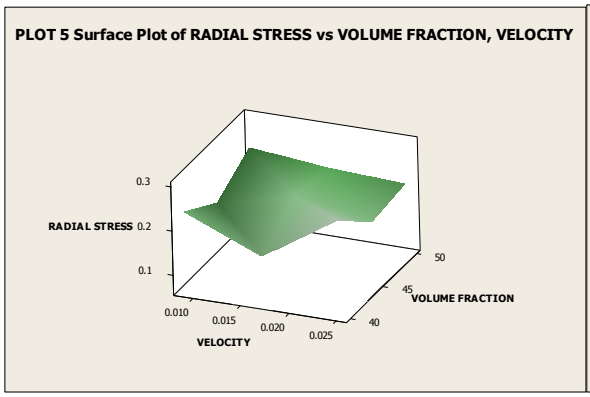

Figure No. 56

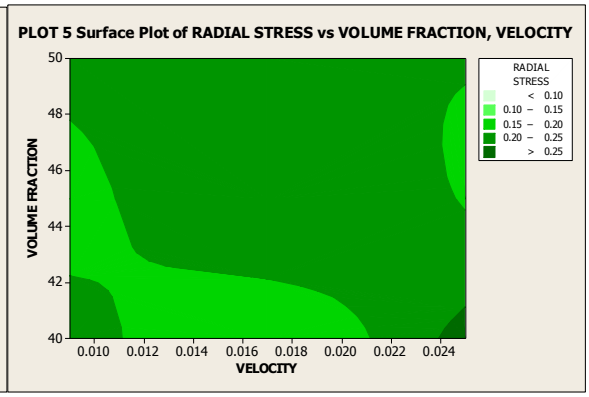

Figure No. 57

The 3D contour plot of radial stress vs. interaction of volume fraction and velocity is presented in Fig. no. 56 which show the plot increases at the middle region of velocity and volume fraction. The 2D contour plot of radial stress vs. interaction of volume fraction and velocity is shown in Fig. no. 57.

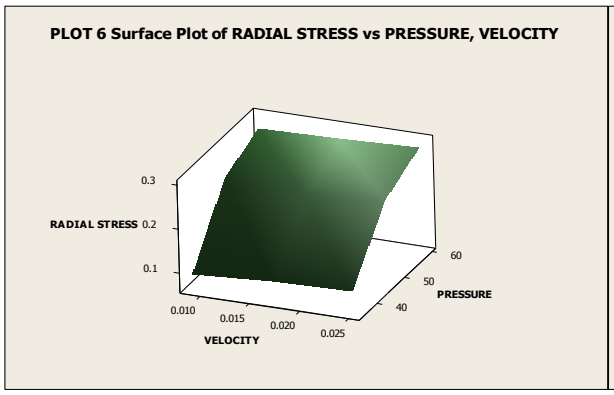

Figure No. 58

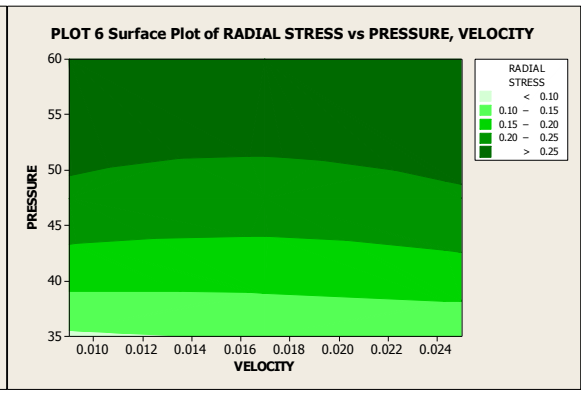

Figure No. 59

The 3D contour plot of radial stress vs. interaction of velocity and pressure is presented in Fig. no. 58 which show the plot increases with increasing by pressure and remains almost constant with velocity. The 2D contour plot of radial stress vs. interaction of velocity and pressure is shown in Fig. no. 59.

Indentation depth:

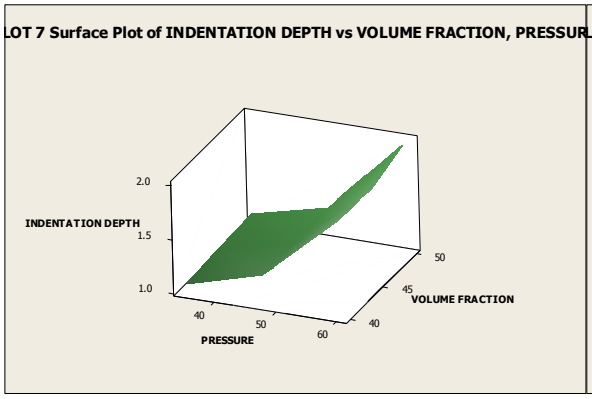

Figure No. 60

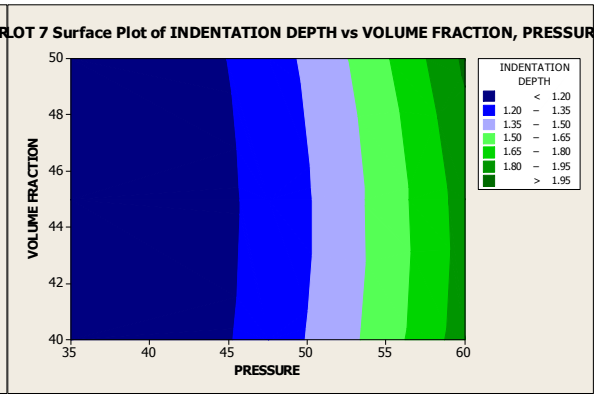

Figure No. 61

The 3D contour plot of indentation depth vs. interaction of volume fraction and pressure is presented in Fig. no. 25 which show the plot increases with increasing in pressure and remains constant with volume fraction. The 2D contour plot of indentation depth vs. interaction of volume fraction and pressure is shown in Fig. no. 26.

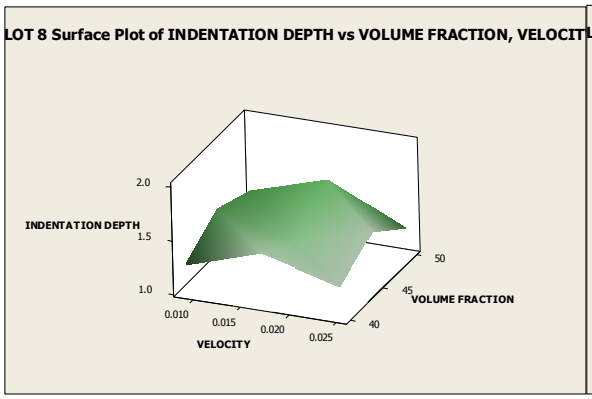

Figure No. 62

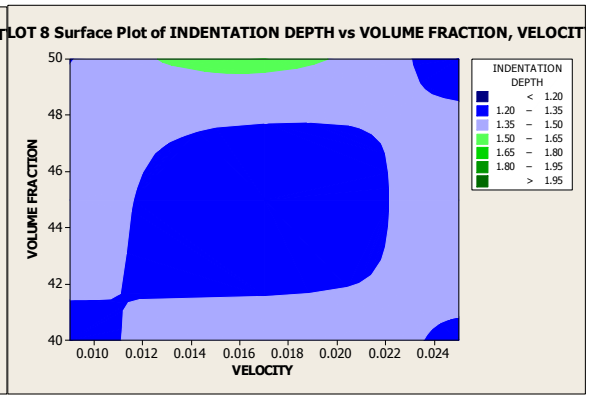

Figure No. 63

The 3D contour plot of indentation depth vs. interaction of volume fraction and velocity is presented in Fig. no. 62 which show the plot decreases with respect to the middle region of velocity and volume fraction. The 2D contour plot of indentation depth vs. interaction of volume fraction and velocity is shown in Fig. no. 63.

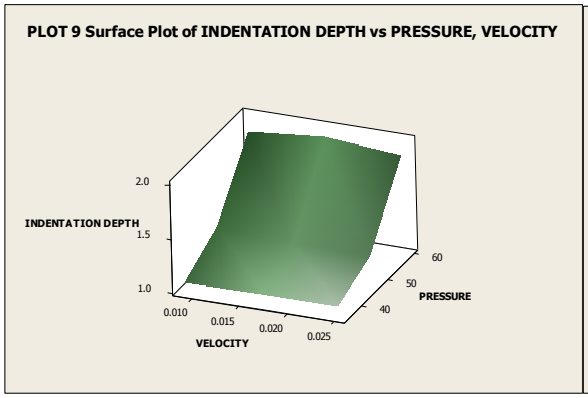

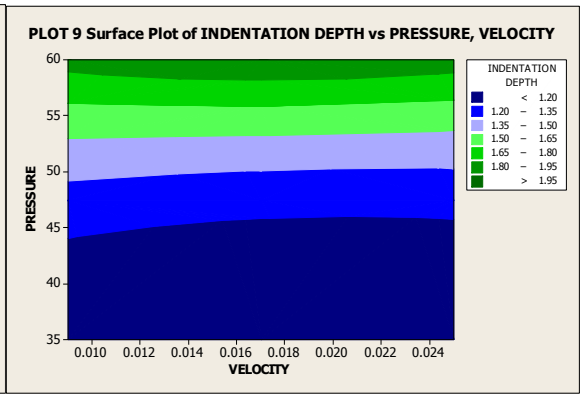

Figure No. 64 Figure No. 65

The 3D contour plot of indentation depth vs. interaction of velocity and pressure is presented in Fig. no. 64 which show the plot increases with increasing by pressure and remains constant with velocity. The 2D contour plot of indentation depth vs. interaction of velocity and pressure is shown in Fig. no. 65.

Chapter 6

Conclusion

The present study develops CFD simulation of AFM in a flat workpiece and in a pipe taking different input parameters and then the results are verified. The present study also develops optimization for AFM process of Al. alloy using response surface method. It is found that all the three machining parameters and some of their interactions have significant effect on outputs considered in the present study. Finally, an attempt has been made to estimate the optimum machining conditions to produce the best possible output within the experimental constraints.

- From CFD analysis it is found the axial stress, radial stress at the workpiece surface and then the axial force and normal forces area calculated.
- Material removal rate also calculated from this simulation.
- The optimal condition of input variables are at 50 % of volume fraction, 60 bar of pressure and 0.017 m/s of velocity in this study and also get maximum value of each output responses.
- The ANOVA revealed that the pressure is the most significant factor influencing the response variables examined.
- Additionally, the volume fraction and velocity also provided secondary contribution to the out responses.
- The reduced linear models developed using RSM were reasonably perfect and can be used for prediction within the limits of the factors investigated.

Chapter 7

Refrences

[1] Gorana, V.K., Jain, V.K., Lal, G.K., 2004, Experimental investigation into cutting forces and active grain density during abrasive flow machining, International Journal of Machine Tool & Manufacture, Vol. 44, pp. 201-211.

[2] Gorana V. K, Jain V. K. and Lal G. K. "Prediction of surface roughness during abrasive flow machining", *The International Journal of Advanced Manufacturing Technology*, 2006,(31):258-267

[3] Jain R.K, Jain V.K, Simulation of surface generated in abrasive flow machining, Robotics and Computer Integrated Manufacturing 15 (1999) 403–412.

[4] Lal G.K., Forces in vertical surface grinding, International Journal of Machine Tool Design Research 8 (1968) 33–43.

[5] Jain R.K, Jain V.K, Dixit P.M. Modelling of material removal and surface rough-ness in abrasive flow machining process, International Journal of Machine Tools & Manufacture 39 (1999) 1903–1923

[6] Jha. S, Jain V.K, Design and development of the magneto rheological abrasive flow finishing process, International Journal of Machine Tools & Manufacture 44 (2004) 1019-1029.

[7] Jha S, Jain V.K, Modelling and simulation of surface roughness in magneto rheological abrasive flow finishing (MRAFF) process, Wear 261 (2006) 856–866.

[8] Das M, Jain V. K and Ghoshdastidar P.S Computational fluid dynamics simulation and experimental investigations into the magnetic-field-assisted nano-finishing process (2012).

[9] Jayswal S.C, Jain V.K, Dixit P.M. Modelling and simulation of magnetic abrasive finishing process, International Journal of Advanced Manufacturing Technology 26 (2005) 477–490.

[10] Singh, S., Shan, H.S., Kumar, P., 2002, Wear behaviour of materials in magnetically assisted abrasive flow machining, Journal of Materials Processing Technology, Vol. 128, pp. 155- 161.

[11] Rhoades L.J, Abrasive flow machining, Manufacturing Engineering (1988) 66-82.

[12] Rhoades L.J, Abrasive flow machining with not-so-silly putty, Metal Finishing July (1987) 22-28.

[13] Rhoades L.J, Abrasive flow machining: a case study, Journal of Material Processing Technology 28 (1991) 101-117.
[14] Rhoades, L.J., 1989, Abrasive Flow Machining, Technical Paper of the Society of Manufacturing Engineers (SME), MR89 – 145.
[15] Przylenk K, AFM—a process for surface finishing and deburring of the workpiece with a complicated shape by means of an abrasive laden medium, PED, 22ASME, NewYork,1986, pp. 98-116.
[16] Williams R.E, Rajurkar K.P, Metal removal and surface finish characteristics in abrasive flow machining, PED, 38ASME, New York, 1989, pp. 87–104.
[17] Loveless T.R, Willams R.E, Rajurkar K.P, A study of the effects of abrasive flow finishing on various machined surfaces, Journal of Material Processing Technology 47 (1994) 127-142.
[18] Williams R.E. Rajurkar K.P, Stochastic modeling and analysis of abrasive flow machining, Transactions of the ASME, Journal of Engineering for Industry 114 (1992) 7481.
[19] Williams R.E, Acoustic emission characteristics of abrasive flow machining, Transactions of the ASME120 (1998) 264–271.
[20] Williams, R.E., Rajurkar, K.P., Rhoades, L. J., 1989, Performance Characteristics of Abrasive Flow Machining, Technical Paper of the Society of Manufacturing Engineers (SME), MR89-806.
[21] William R.E, Rajurkar K.P. Monitoring of abrasive flow machining process using acoustic emission, S.M. Wu Symposium, vol. I, 1994, pp. 35–41.
[22] Fletcher A.J, Hull J.B, Mackie J, Trengove S.A, Computer modeling of abrasive flow machining process, Proceedings of the 210 V.K. Gorana et al. / International Journal of Machine Tools & Manufacture 44 (2004) 201–211 International Conference on Surface Engineering, Toronto, 1994, pp. 31-47, 1990, pp. 584-611.
[23] Kukreja T.R and Mohan Rakesh "A case study of EPDM rubber media utilized in the abrasive flow machining process'Rubber India 55 (2003). pp.9 $^{-11}$
[24] Macosko C.W. Rheology Principles, Measurement & Applications, VCH Publishers Inc., New York, 1994.
[25] Beverly C.R, Tanner R.I. Numerical analysis of three-dimensional Bingham plastic flow, Journal of Non-Newtonian Fluid Mechanics 42 (1992) 85–115.
[26] Bird R.B, Stewart W.E, Lightfoot E.N, Transport Phenomena, Wiley, New York, 1960.
[27] Fang,L, Zha, J., Sun, K, Zheng, D, Ma, D., 2009, Temperature as sensitive monitor for efficiency of work in abrasive flow machining, Wear, Vol. 266, pp. 678-687.

[28] Uhlmann,E, Szulczynski, H., 2005, Precise finishing of inner contours with abrasive flow machining, International Journal for Manufacturing Science & Technology, Vol. 7 (2), pp. 33-39.

[29] Uhlmann, E, Mhotovic, V, Coenen, A., 2009, Modelling the abrasive flow machining process on advanced ceramic materials, Journal of Materials Processing Technology, Vol. 209, pp. 6062- 6066.

[30] Sankar, M.R., Jain, V.K, Ramkumar, J., 2007, Abrasive flow machining (AFM): An Overview, psgias/smart_machine_tools/V.K.Jain.pdf, 22.11.2011.

Fig. 10: FAX for different end piece geometries at 45 bar piston

[31] Junye Li, Liu Weina, Yang Lifeng, Li Chun, Liu Bin, Wu Haihong and Sun Xiaoli Design and Simulation for Mico-hole Abrasive Flow Machining (2009) 815-819.

[32] Tzeng Hsinn-Jyh, Yan Biing-Hwa, Hsu Rong-Tzong, and Lin Yan- Cherng. "Self-modulating abrasive medium and its application to abrasive flow machining for finishing micro channel surfaces", *TheInternational Journal of Advanced Manufacturing Technology*, 2007,(5):1163-1169

[33] Tsai M. J, Huang J. F. "Efficient automatic polishing process with a new compliant abrasive tool", *The International Journal of Advanced Manufacturing Technology*, 2006,(30),817-827

[34] Jain N. K, Jain V. K, and Jha S. "Parametric optimization of advanced fine-finishing processes", *The International Journal of Advanced Manufacturing Technology*, 2007,(34): 1191-1213

[35] Perry, W.B., 1975, Properties and Capabilities of low-pressure abrasive flow media, Technical Paper of the society of Manufacturing Engineers (SME), MR75-831.

[36] Borchers, J., 1980, Why? Abrasive Flow Deburring, Technical Paper of the Society of Manufacturing Engineers (SME), MR80 – 101.

[37] R.H. Myers, D.C. Montgomery, Response Surface Methodology-Process and Product Optimization Using Robust Design, Wiley Series in Probability and Statistics, Wiley, New York, 1995. pp. 318–321.

[38]D.J. Whitehouse, Handbook of Surface Metrology, Institute of Physics Publishing, Bristol, UK, 1994

[39] Design-Expert Software, Version 6, User's Guide, Technical Manual, Stat-Ease Inc., Minneapolis, MN, 2000